Precise measurement of the $e^+e^- \to \pi^+\pi^-(\gamma)$ cross section

Michel Davier, Anne-Marie Lutz, Bogdan Malaescu, Zhiqing Zhang
Léonard Polat, **Andrés Pinto**

08/09/2025

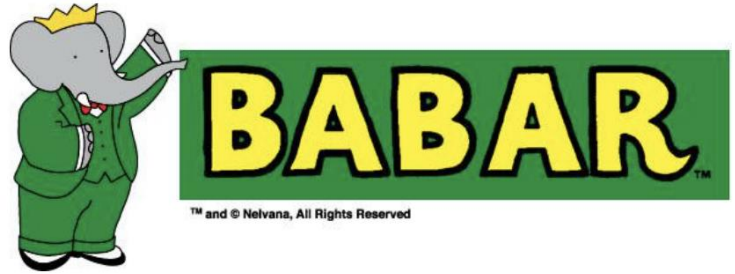

8th Plenary workshop of the Muon g-2 Theory Initiative 2025

Motivation

- The muon anomalous magnetic moment a_μ is sensitive to hadronic vacuum polarization (HVP).
- The dominant input (≈73%) comes from $e^+e^- \to \pi^+\pi^-$.

- Current tensions:
  - Tensions among inputs of the dispersive approach
  - Dispersion approach vs direct experimental measurements.
  - Dispersion approach vs lattice QCD predictions.
- Resolving these discrepancies is crucial for testing the Standard Model.
- BaBar performed a first a_μ measurement in 2009 with **partial data**.
- Need new precise and independent measurements to resolve the situation.

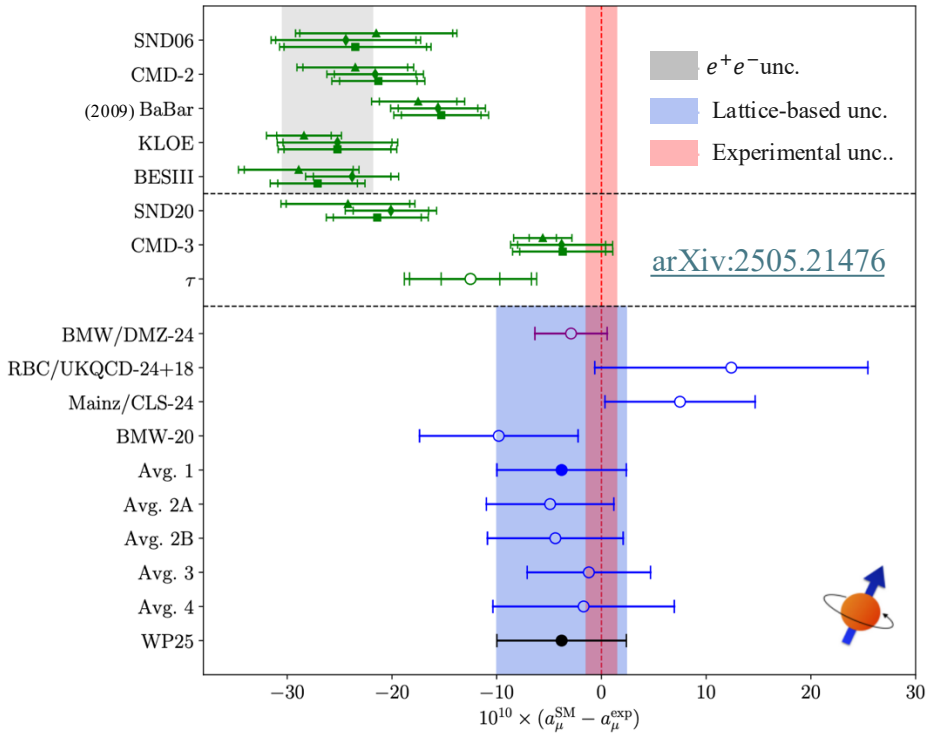

arXiv:2505.21476

Phys. Rev. D 109 (2024) 112002

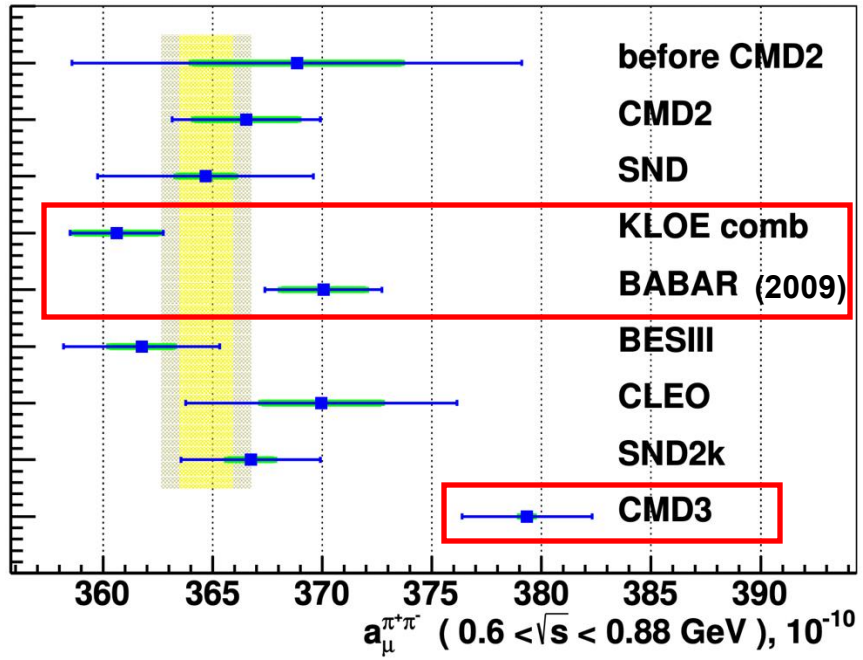

The BaBaR experiment

- **PEP-II collider (SLAC, USA):**
  - Asymmetric $e^+(3\,\text{GeV}) - e^-(9\,\text{GeV})$
  - Operated from 1999 to 2008 at Y(4S/3S/2S) resonance energies
  - Collected $\mathbf{424\ fb^{-1}}$ at ($\sqrt{s} = 10.58\,\text{GeV}$) + $\mathbf{36\ fb^{-1}}$ off-resonance
- **Strategy:**
  - Initial State Radiation (ISR) to probe a wide range of effective energies
- **Signals studied:**
  - $e^+e^- \to \mu^+\mu^-(\gamma_{\text{ISR}})$
  - $e^+e^- \to \pi^+\pi^-(\gamma_{\text{ISR}})$
  - Simulated with Phokhara9.1
- **Backgrounds:**
  - $e^+e^-\gamma,\ K^+K^-(\gamma_{\text{ISR}}),\ q\bar{q}\ (u,d,s,c),\ \tau^+\tau^-$, multipion ISR processes ($X\gamma_{ISR}$ for $X = n\pi + m\pi^0, \ldots$)

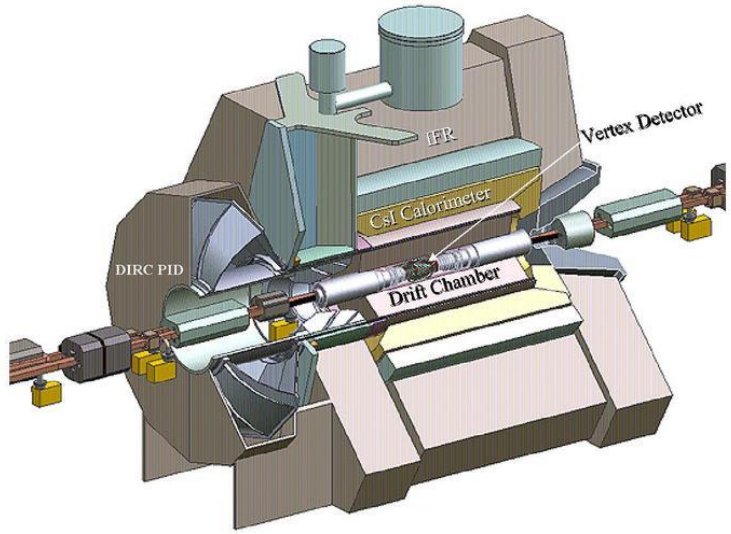

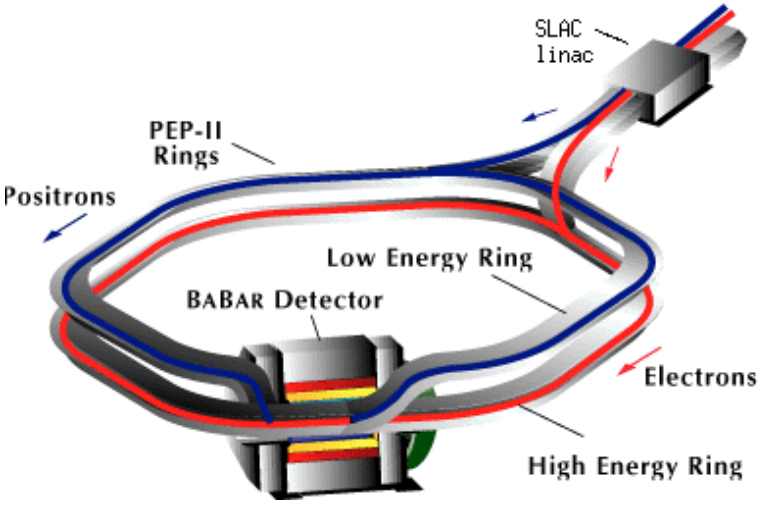

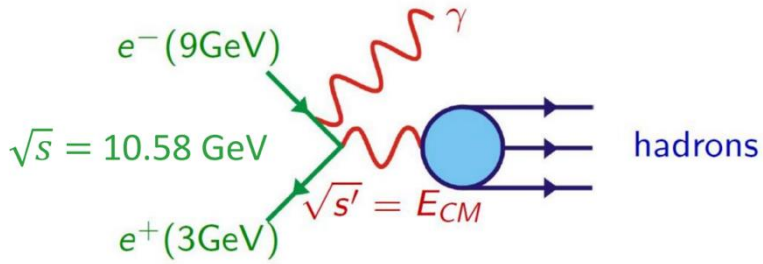

BABAR methods for measuring $e^+e^- \to \pi^+\pi^-, \mu^+\mu^-$

- **ISR (Initial State Radiation):**
  - Full mass spectrum obtained from one dataset via large-angle ISR photons
  - Good detector acceptance for final states
- **$\pi\pi/\mu\mu$ ratio method:**
  - Cancels common systematics (luminosity, ISR photon efficiency, vacuum polarization)
  - Relies on well-understood $\mu\mu$ QED process as reference
- **Additional radiation (NLO & beyond):**
  - Loose selection includes ISR/FSR photons
  - NLO ISR and FSR measured directly in data
  - NNLO hard contributions studied in 2023 (Phys. Rev. D 108, L111103 (2023))
  - Method largely independent of generator limitations (Phokhara restricted to NLO)

Lowest-order (LO) ISR

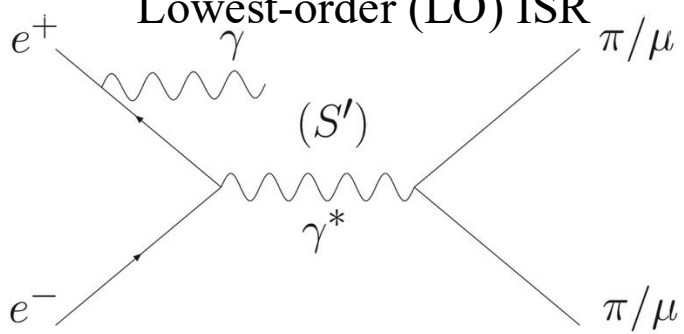

Lowest-order (LO) FSR

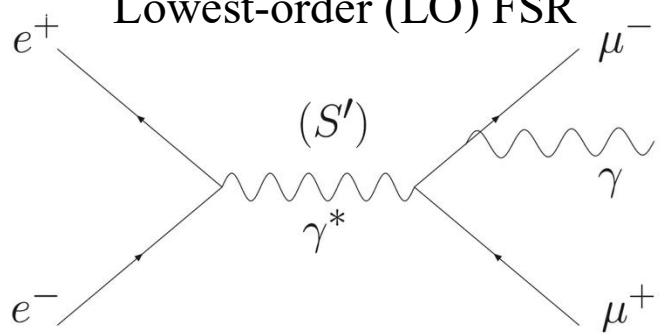

Next-to-leading-order (NLO) ISR

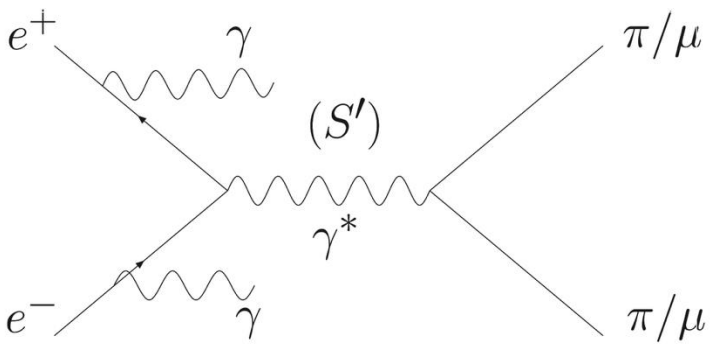

Next-to-leading-order (NLO) FSR

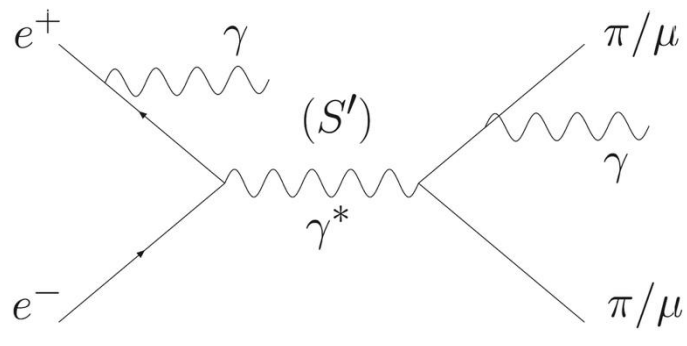

2009 analysis vs 2025 analysis

- **2009 Analysis (Phys.Rev.Lett. 103 (2009) 231801)**
  - Data: partial 232 fb^{-1} (Y(4S))
  - π/μ separation via **particle ID (PID)** → main source of systematics
  - Track cut: $p > 1$ GeV/c
  - Signal MC: AfkQED
  - Systematic uncertainty ≈ 0.5%
- **2025 Analysis**
  - Data: full 460 fb^{-1} **New method** (angular fit on $|\cos\theta^*|$) → no PID required
  - Track cut: $p_T > 0.1$ GeV/c, higher statistics
  - Signal MC: Phokhara9.1
  - Blind analysis with reduced systematics
- **Main improvements (2025):**
  - ×2 larger luminosity
  - Lower momentum threshold
  - Different, more robust π/μ separation method

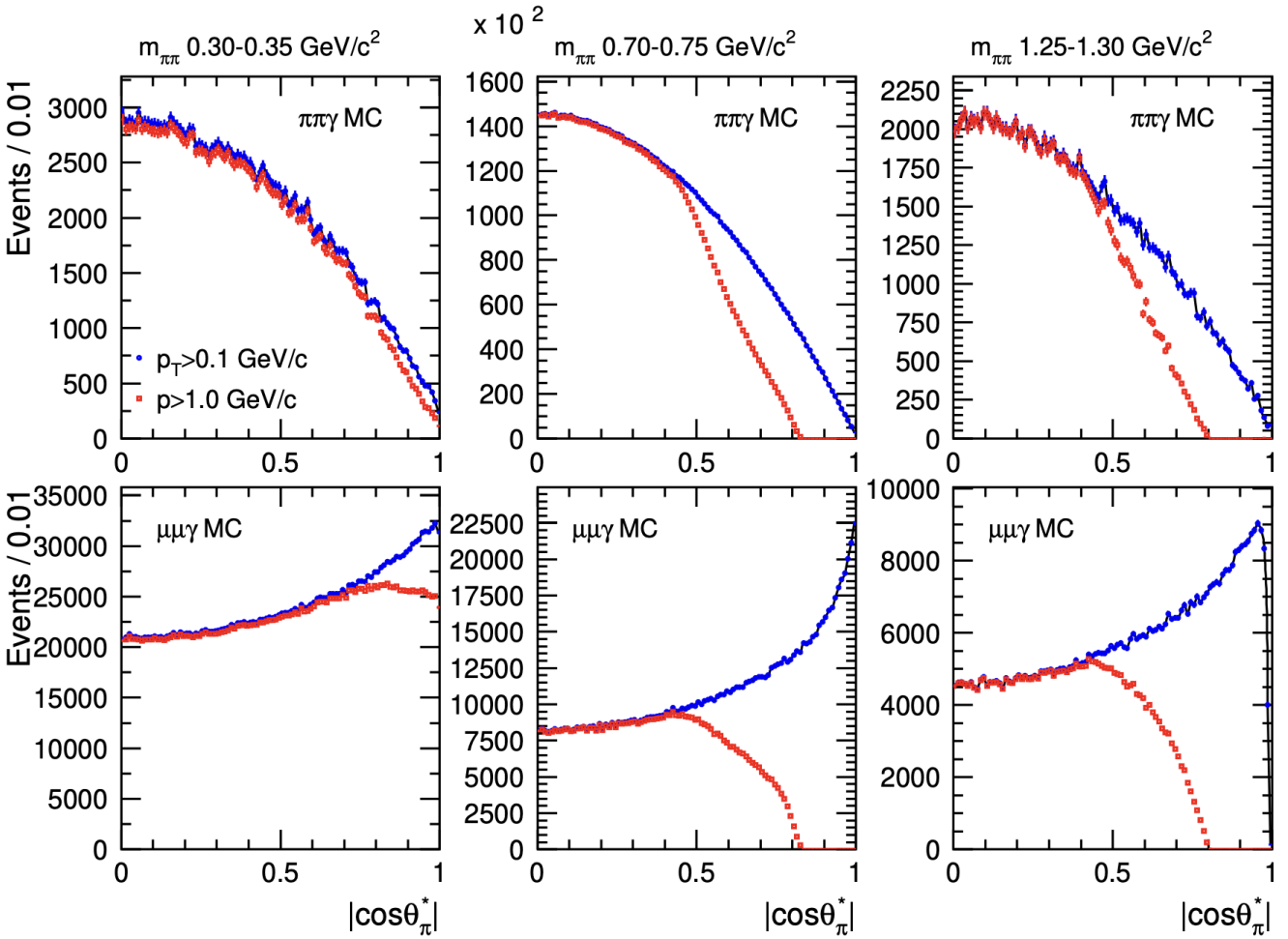

θ^*: angle between negative charged track and γ_{ISR} in 2-track CM frame

Signal event selection

- **ISR photon:** $0.35 < \theta_\gamma < 2.4$ rad, $E_\gamma > 3$ GeV, $E_\gamma^* > 4$ GeV
- **Two opposite-charge "super-good" tracks:**
  - $p_T > 0.1$ GeV/c, $0.4 < \theta < 2.45$ rad
  - ≥ 15 DCH hits, DOCA < 5 mm, $|d_z| < 6$ cm
- Allow additional photons and other quality tracks per event.
- Vertex constraint: $V_{xy} < 0.5$ cm
- Veto electron contamination
- Two NLO radiation fits per event (small-angle ISR $\boldsymbol{\gamma_{ISR}\gamma_{SA}}$ & large-angle ISR/FSR $\boldsymbol{\gamma_{ISR}\gamma_{LA}}$)

Background Control and Suppression

- Optimized 2D $-\chi^2$ selection using BDT in three mass regions
- With all selections, residual background < 5%
- Dedicated studies for background normalization: $2\pi\pi^0$, uds, and $\tau\tau$
- Other backgrounds estimated from MC simulations normalized to BaBar cross-section measurements

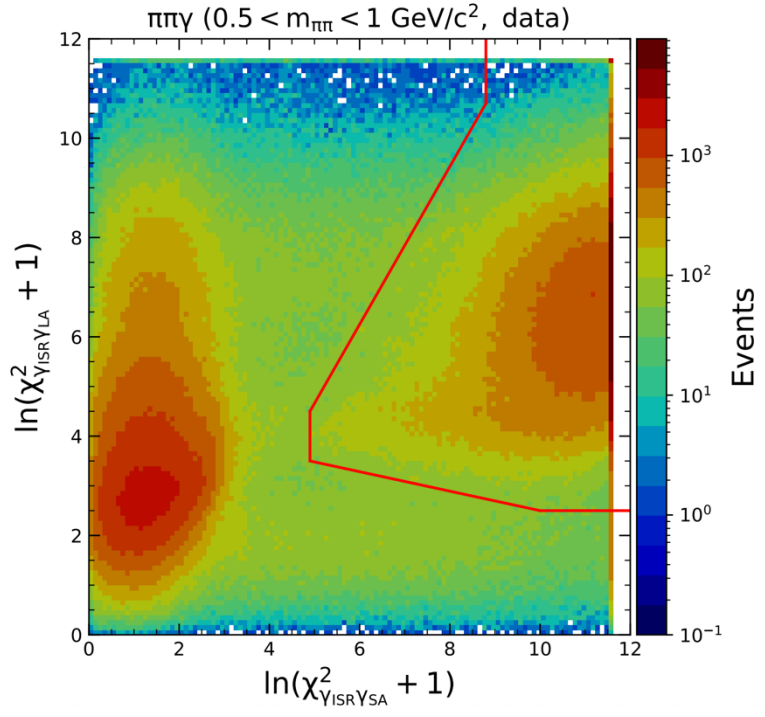

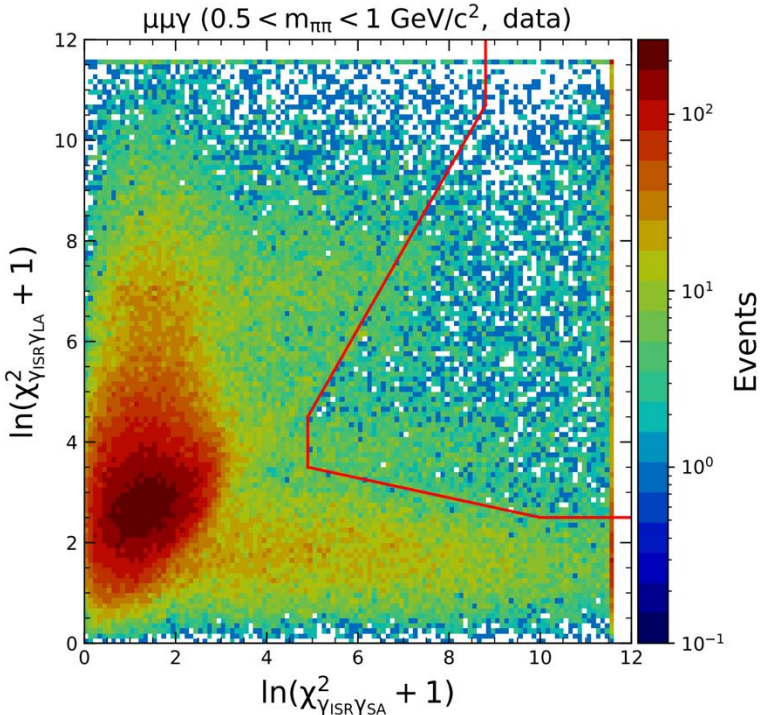

Template fits to separate $\mu\mu/\pi\pi$ final states

- $|\cos\theta^*_\pi|$distributions on background-subtracted data are fitted using **templates**:
  - $\boldsymbol{\pi\pi\gamma}, \boldsymbol{\mu\mu\gamma}$ and $\boldsymbol{KK\gamma}$ obtained from MC signal + data/MC corrections
  - $\boldsymbol{ee\gamma}$ obtained from Data-driven (cut-based and BDT selections)
- **Templates need to be corrected for:**
  - V_{xy} selection efficiency
  - 2D-χ^2 selection efficiency
  - Trigger and tracking efficiencies
- Trigger and tracking corrections are **blinded** until the end of the analysis.
- Fits done twice: pion mass ($m_{\pi\pi}$) & muon mass ($m_{\mu\mu}$) charged track hypotheses
- Data $|\cos\theta^*_\pi|$ distribution is adjusted by linear combination of templates in >300 bins
- For each mass bin, the fit strategy is as follows:
  - $\boldsymbol{|\cos\theta^*_\pi| \in [0.9, 1.0]}$ **:** to obtain $ee\gamma$ normalization (template from data)
  - $\boldsymbol{|\cos\theta^*_\pi| \in [0.0, 0.9]}$ **:** separate ππ / μμ (and KK for low mass)
  - Extrapolate to $|\cos\theta^*_\pi| = 1 \rightarrow$ full ππ/μμ yields
- Fit fractions ($f_{\pi\pi}, f_{\mu\mu}, f_{KK}, f_{ee\gamma}$) extracted from template shapes
- Mass spectra **blinded**, obtained after extrapolation of final fit results to $|\cos\theta^*_\pi| = 1$

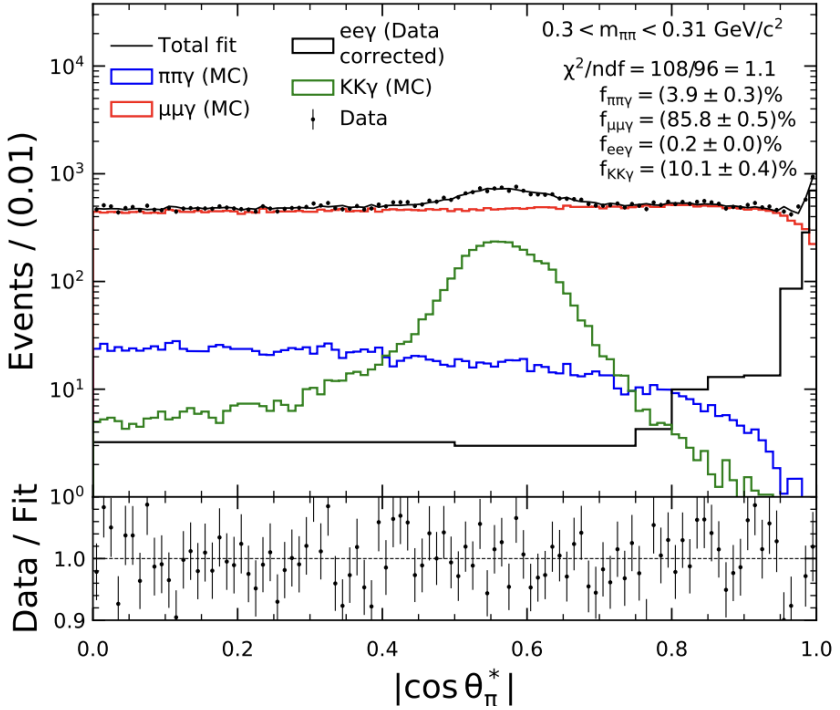

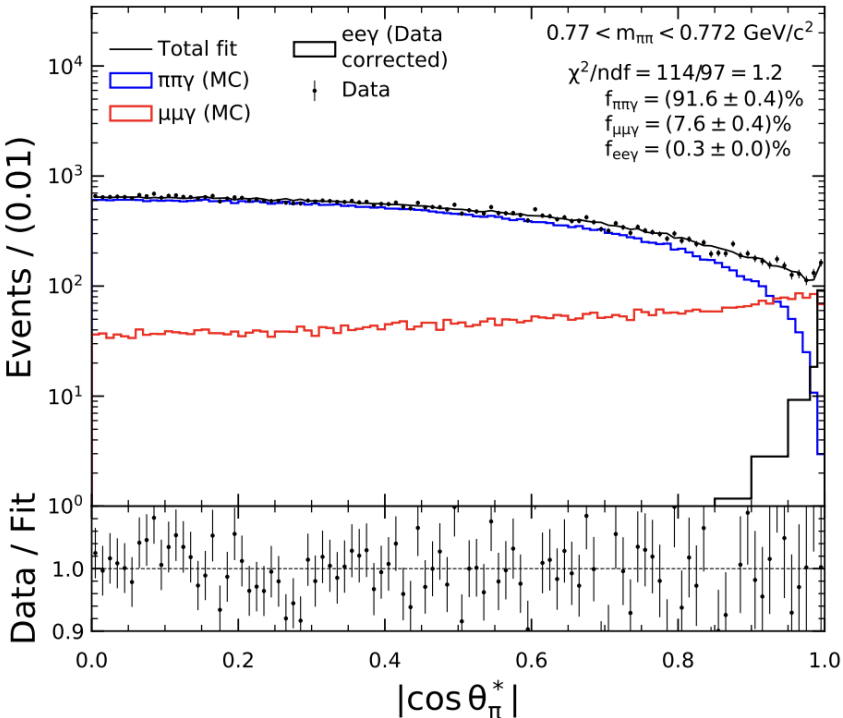

Data-driven eeγ template distribution

- The Monte Carlo prediction is found to be unreliable → the $ee\gamma$ templates are derived using a data-driven method.
- Pure $ee\gamma$ background selected from data using cut- and BDT-based selections.
- Event yields vs. $m_{\pi\pi}$ used to build template normalization.
- Angular distribution ($|\cos\theta^*_\pi|$) extracted as the **template shape.**
- $ee\gamma$ yields from template fits vs mass compared with the initial spectrum.
- Validation of data driven templates.

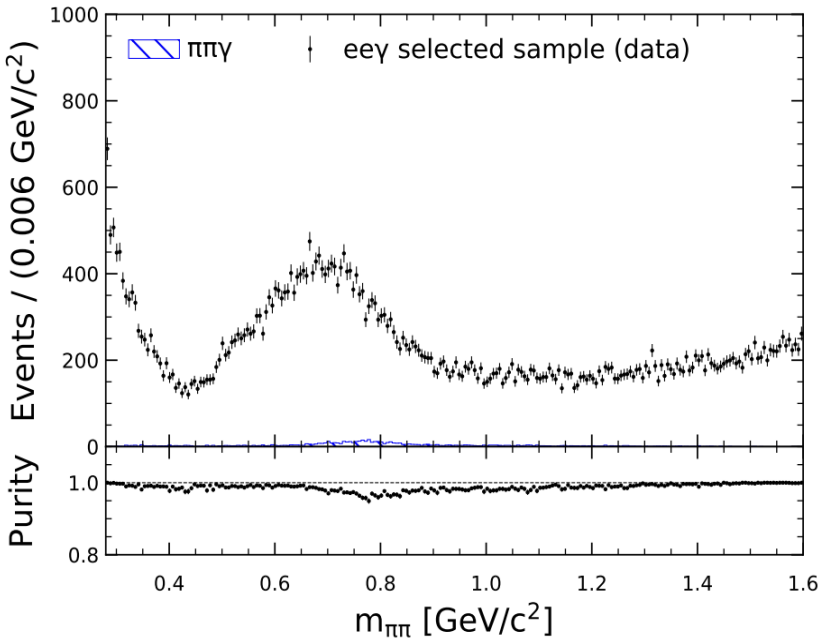

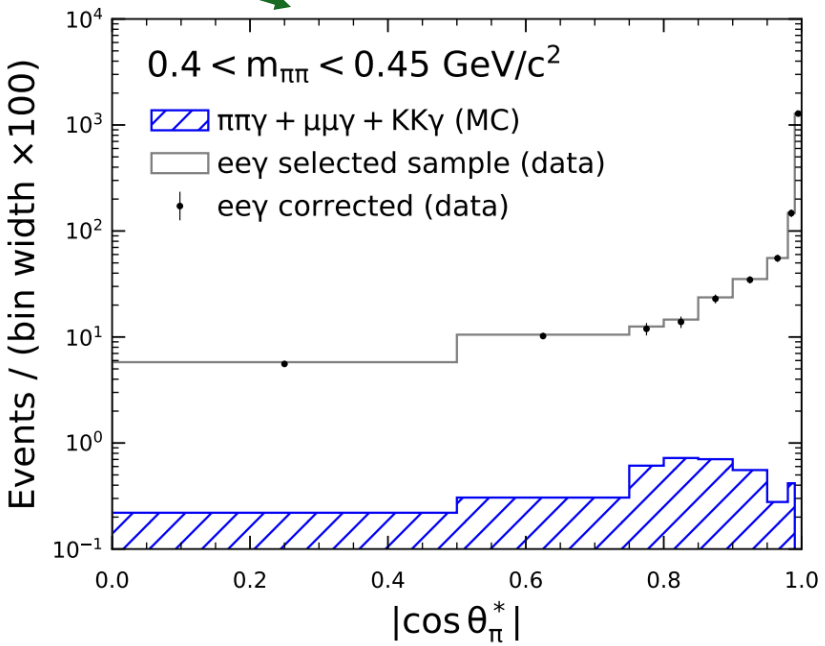

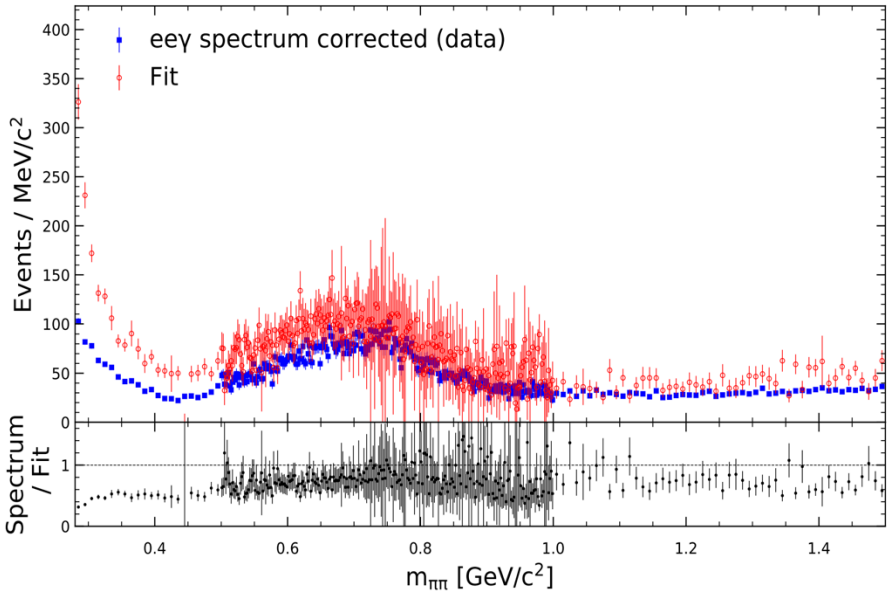

Corrections to Templates and Mass Distributions

- Detailed and dedicated analysis studies of **data/MC differences** on PID-selected muon and pion samples: triggers, tracking, V_{xy}, and 2D$-\chi^2$ selections.
- Efficiency corrections applied:

$$\varepsilon = \varepsilon_{\mathrm{MC}} \left(\frac{\varepsilon^{\mathrm{data}}_{\mathrm{trigger}}}{\varepsilon^{\mathrm{MC}}_{\mathrm{trigger}}} \right) \left(\frac{\varepsilon^{\mathrm{data}}_{\mathrm{tracking}}}{\varepsilon^{\mathrm{MC}}_{\mathrm{tracking}}} \right) \left(\frac{\varepsilon^{\mathrm{data}}_{V_{xy}}}{\varepsilon^{\mathrm{MC}}_{V_{xy}}} \right) \left(\frac{\varepsilon^{\mathrm{data}}_{\chi^2}}{\varepsilon^{\mathrm{MC}}_{\chi^2}} \right)$$

- Additional corrections for pions: fake photons and secondary interactions
- Each correction has two components:
  - Template shape corrections (affect $\pi\pi/\mu\mu$ separation)
  - Mass dependence corrections (affect $\pi\pi$ and $\mu\mu$ spectra)
- **Blinded procedure:** trigger and tracking corrections initially offset (2 offsets for each process)

2D$-\chi^2$ Selection Efficiency

- For muons **clean channel** → background negligible.
- For pions → background ($ee\gamma, 2\pi\pi^0, uds, KK\gamma, etc$) too large.
- Use $\boldsymbol{\mu}$ **2D**$-\chi^2$ **efficiencies** $\epsilon_{\chi^2}^{\mu\mu\gamma}$ **to obtain** to obtain the pion 2D$-\chi^2$ efficiency $\epsilon_{\chi^2}^{\pi\pi\gamma}$:

$$\epsilon_{\chi^2}^{\pi\pi\gamma,\mathrm{data}} = \epsilon_{\chi^2}^{\mu\mu\gamma,\mathrm{data}} + \epsilon_{\chi^2}^{\pi\pi\gamma,\mathrm{MC}} - \epsilon_{\chi^2}^{\mu\mu\gamma,\mathrm{MC}}$$

- Extra correction for pion: Secondary interactions +fake photons are accounted for by an additional correction derived from data/MC comparisons of pion interactions

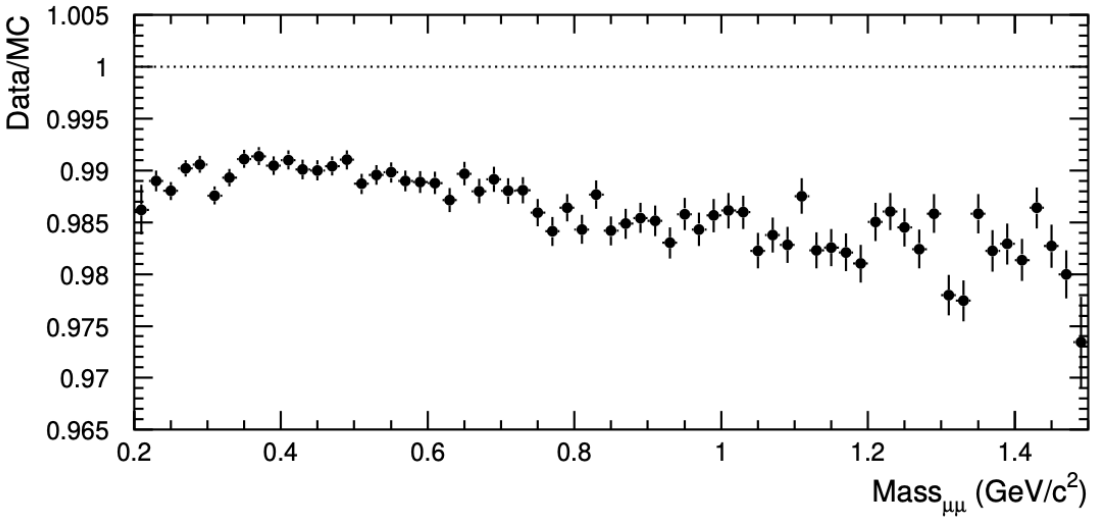

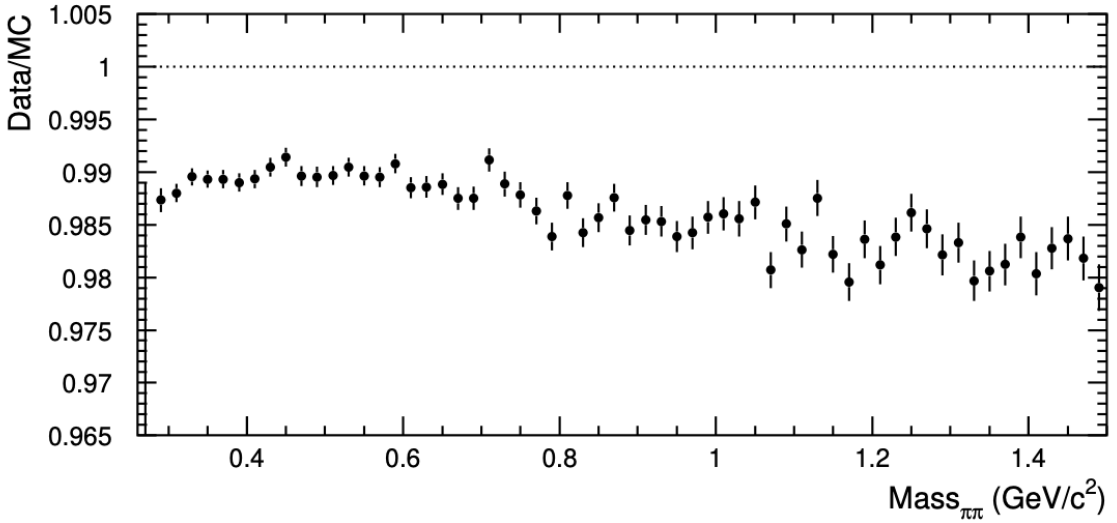

Impact of Tracking Data/MC Corrections

- **Tag-and-probe method** used as in 2009.
- **Correction factor** applied to account for data/MC differences
- μμ fraction is sensitive to small effects in ππ templates (especially near the ρ peak)

- Black error bars = statistical error (pseudo experiments with 1000 toys)
- Red error bars = uncertainties from corrections
- Tracking = **largest correction applied**
- Other corrections (e.g. 2D$-\chi^2$) show compensating effects

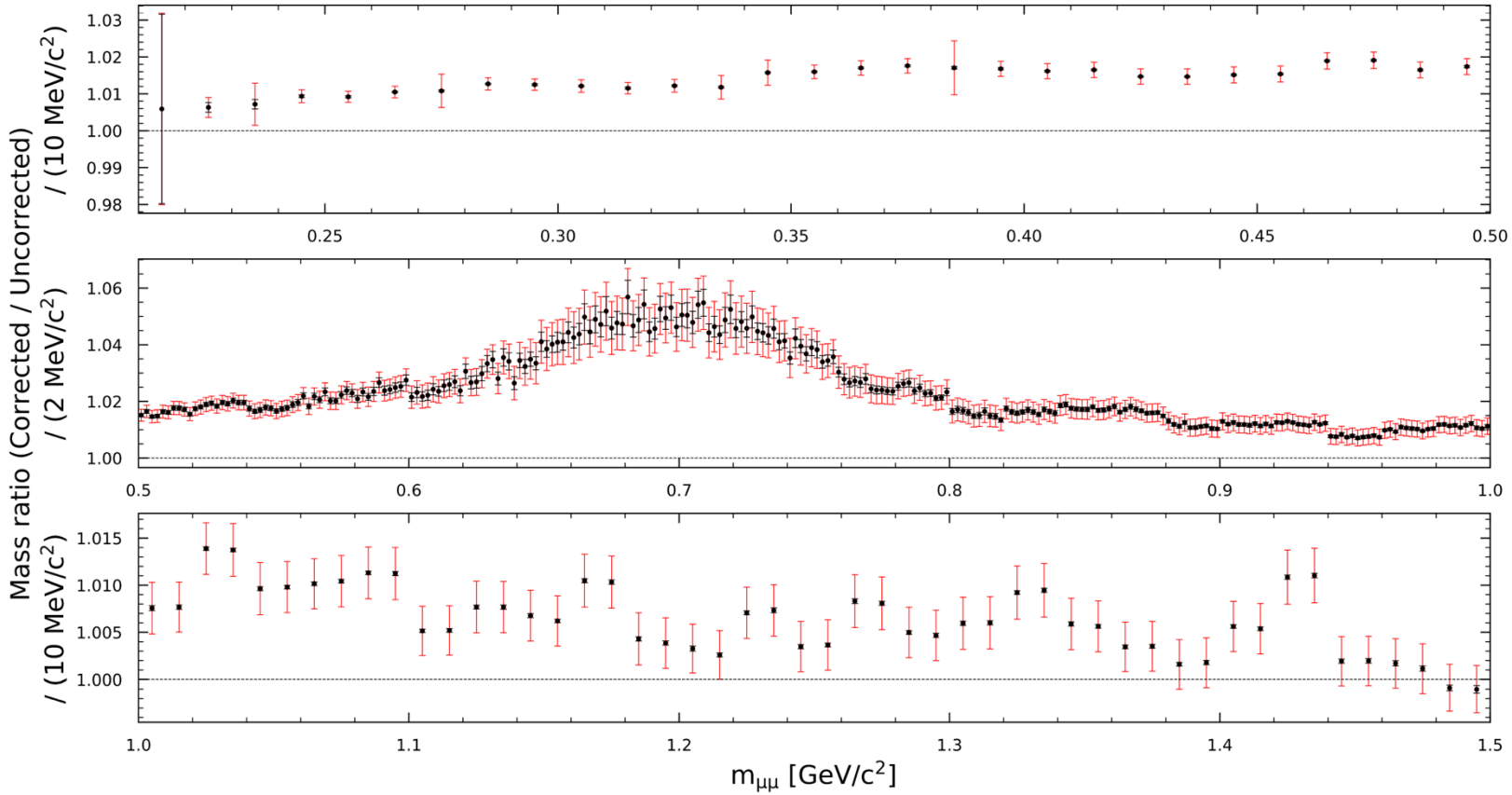

Corrections for the Mass Spectrum

- Combined corrections applied to **Templates** and **Mass spectrum**
- Corrections are fairly flat vs $m_{\mu\mu/\pi\pi}$ showing no strong mass dependence
- Large effect of corrections on mass spectra (below ±5%) that tends to cancel out when combined
- Corrections remain close to unity → small overall impact
- Corrections under control, ensuring reliable m_{XX} spectrum

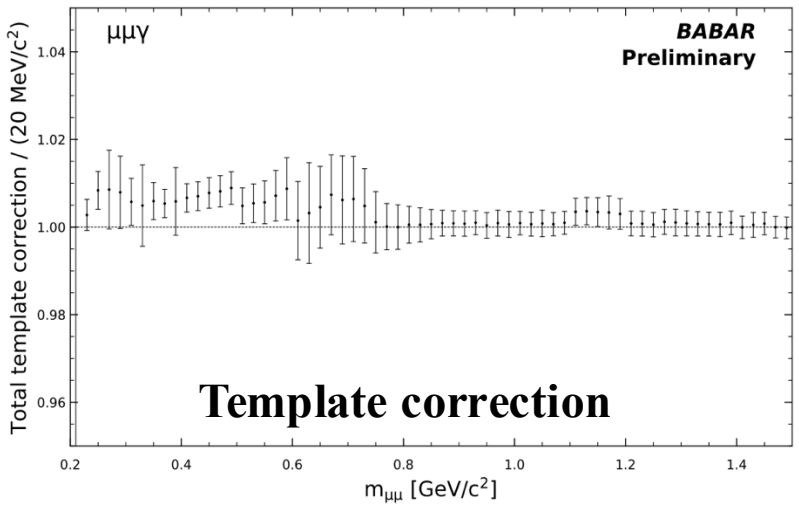

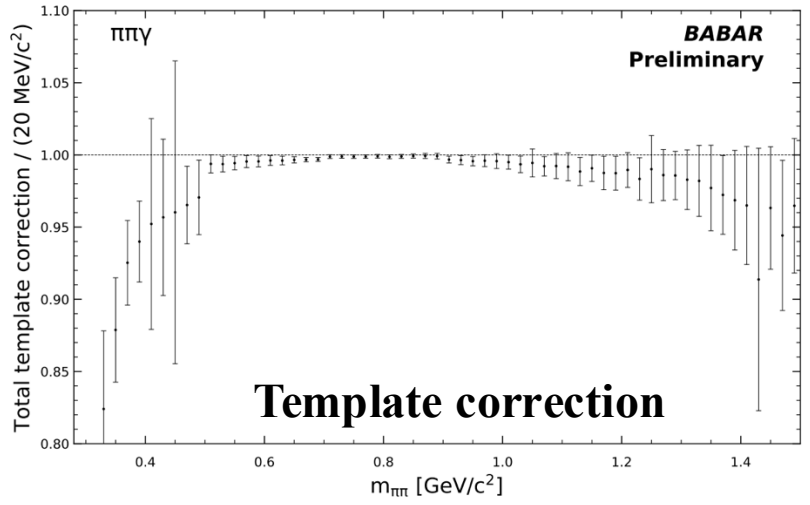

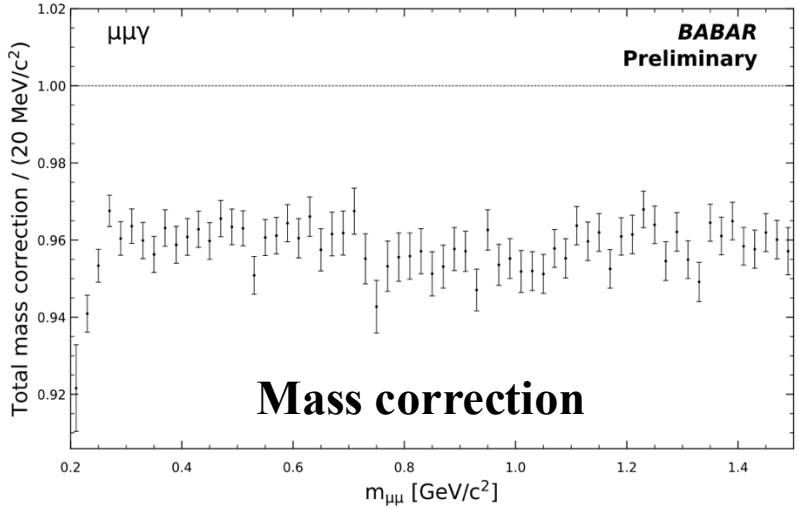

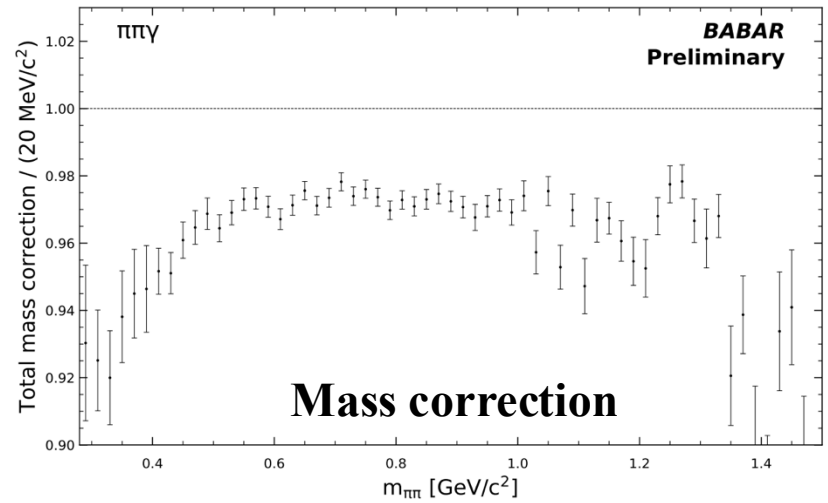

Fitted Mass Spectrum

- Mass spectra obtained from angular fits with blinded absolute corrections (3rd offset).
- Fits performed in:
  - 2 MeV/c^2 bins for 0.5−1.0 GeV/c^2.
  - 10MeV/c^2 bins elsewhere.
- Mass spectra (muon & pion) initially **blinded** with an offset.

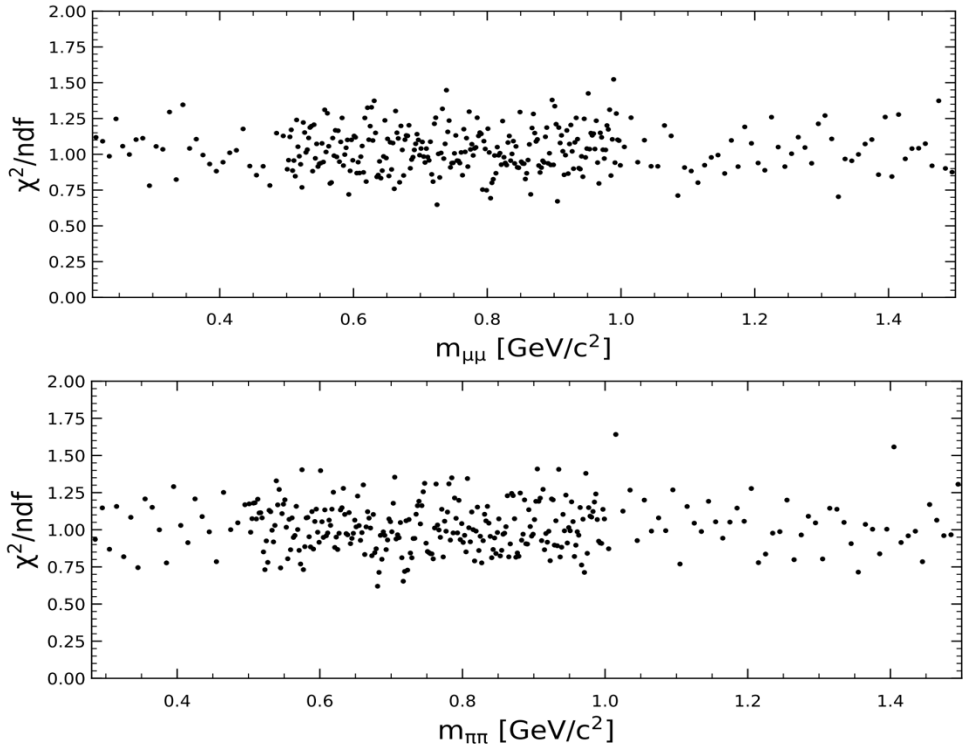

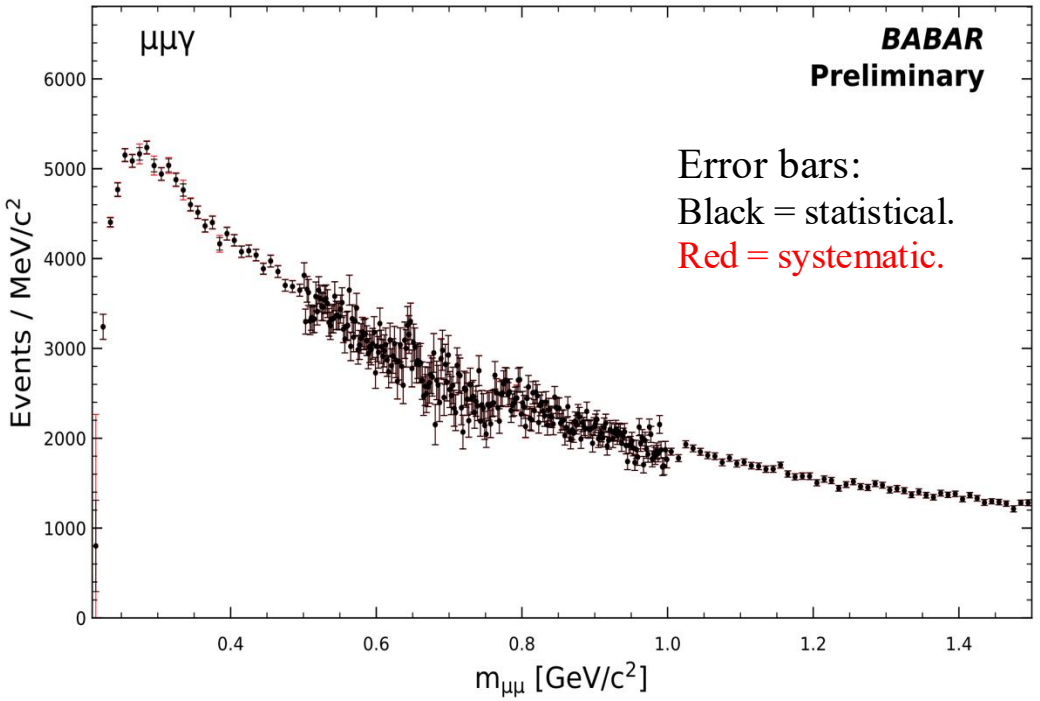

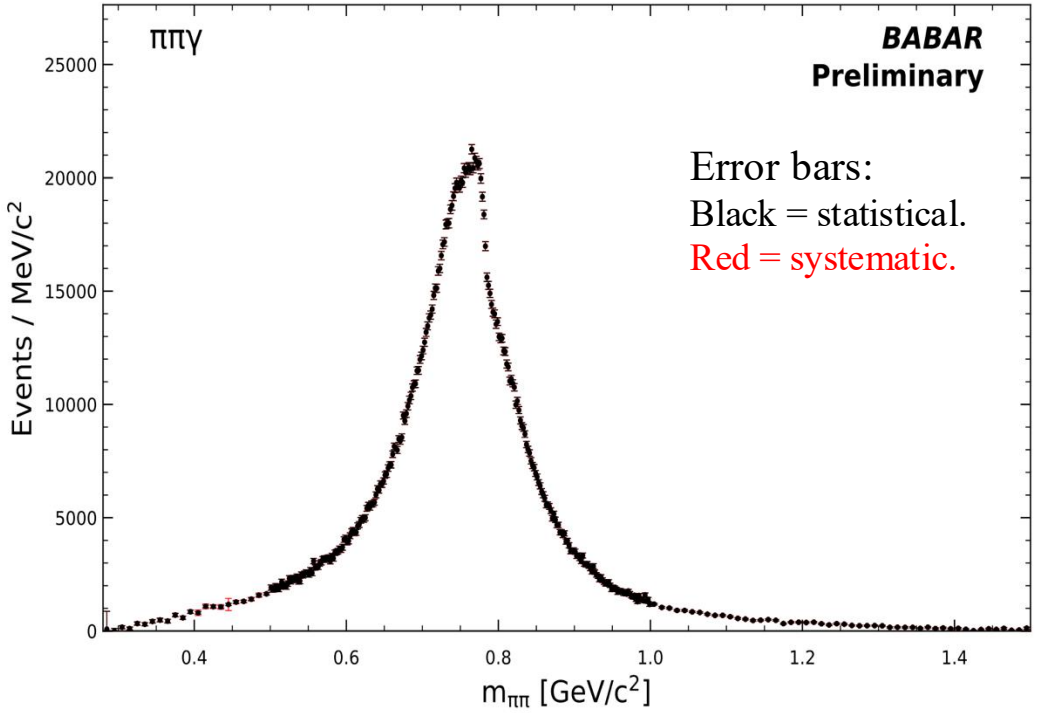

Muon Mass Spectrum vs QED

- $\mu\mu\gamma$ data spectrum can be compared to QED prediction, obtained by correcting the simulated Phokhara spectrum for:
  - ISR photon efficiency
  - NLO–NNLO acceptance correction (<0.03%)
  - Improved vacuum polarization contribution
- Agreement with QED within **0.7%**.
- More precise than 2009 result (±1.1%)
- Confirms robustness of $\pi\pi/\mu\mu$ separation, no major systematic bias

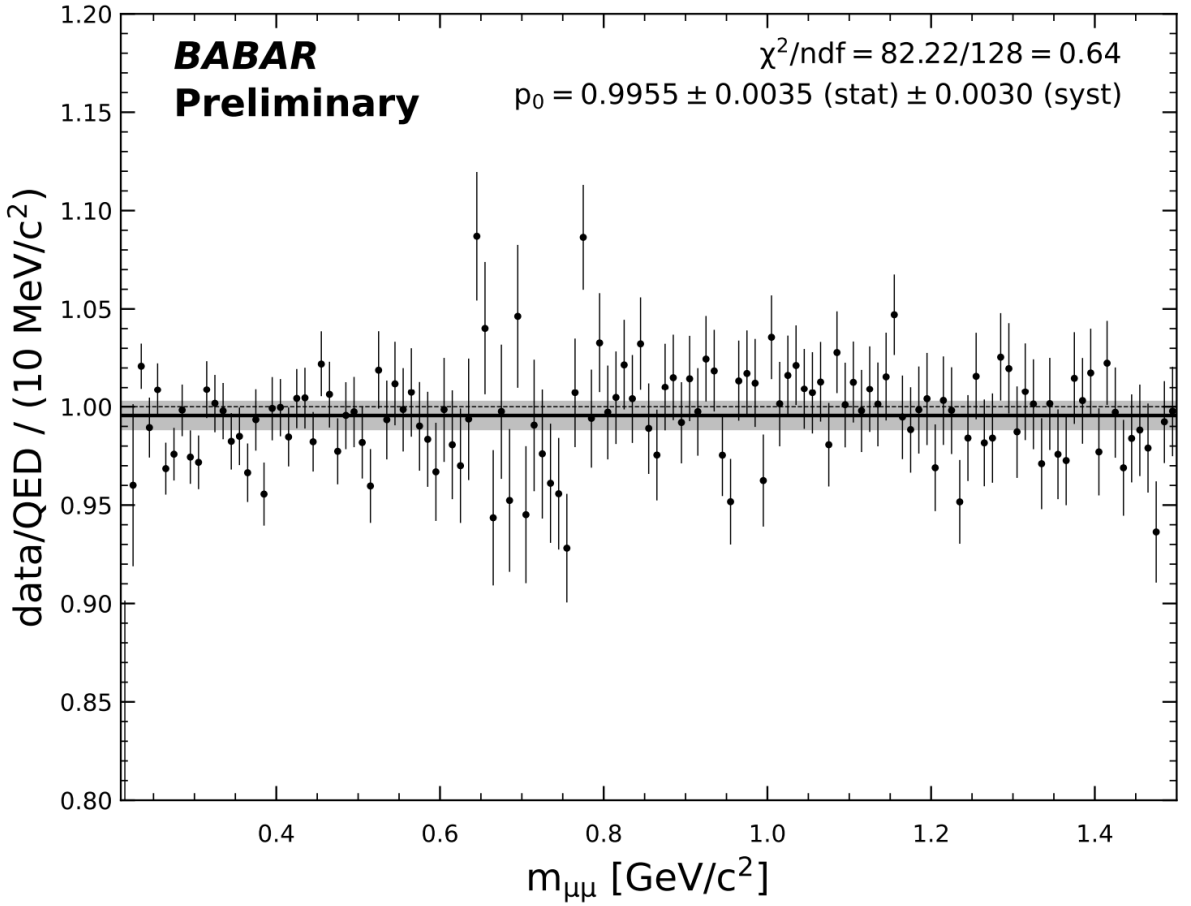

$$2025: R_{\mu\mu} = 0.9955 \pm 0.0035_{stat} \pm 0.0030_{syst} \pm 0.0033_{\gamma\ ISR} \pm 0.0043_{lumi\ ee}$$

data + stat errors on corrections | Syst. related to π/μ separation | ISR photon data/MC efficiency | error on e^+e^- luminosity

$$2009: R_{\mu\mu} = 1.0040 \pm 0.0019_{stat} \pm 0.0043_{syst} \pm 0.0034_{\gamma\ ISR} \pm 0.0094_{lumi\ ee}$$

Unfolding procedure

- Implementation of An iterative, dynamically stabilized method of data unfolding to correct data/MC shape differences.
- Corrects for:
  - Detector resolution.
  - Effect of Final State Radiation (FSR) → shifts $m_{XX} \rightarrow \sqrt{s'}$.
- To perform the unfolding a migration matrix from simulation is constructed using the reconstructed invariant mass m_{XX} and the reduced energy $\sqrt{s'}$ defined as:

$$\sqrt{s'} = \begin{cases} m_{XX} & \text{if.} \quad \theta_{\text{min}}^{\text{true}} > 20^\circ \\ m_{XX\gamma} & \text{if.} \quad \theta_{\text{min}}^{\text{true}} \leq 20^\circ \end{cases}$$

- With $\theta_{\text{min}}^{\text{true}}$ the angle between the FSR/ISR LA photon and the nearest charged track.
- Data-driven studies show systematic uncertainties are small.
- Systematic related to the response matrix ($\theta_{\text{min}}^{\text{true}}$ cut) are included by unfolding the spectrum with different matrices.
- Systematics uncertainties are propagated by $\pm 1\sigma$ variations

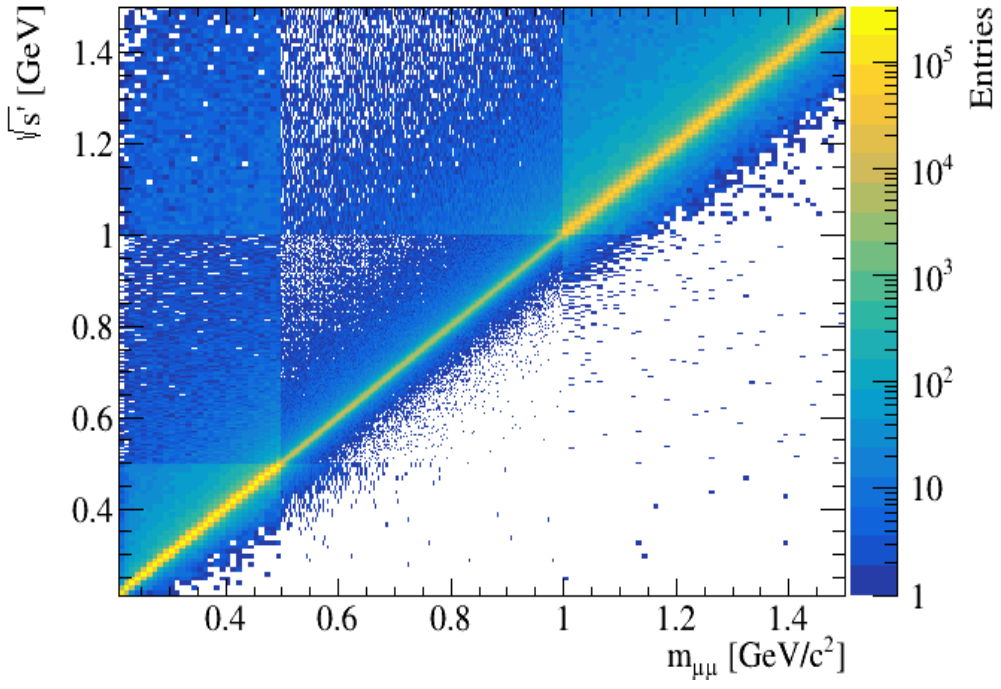

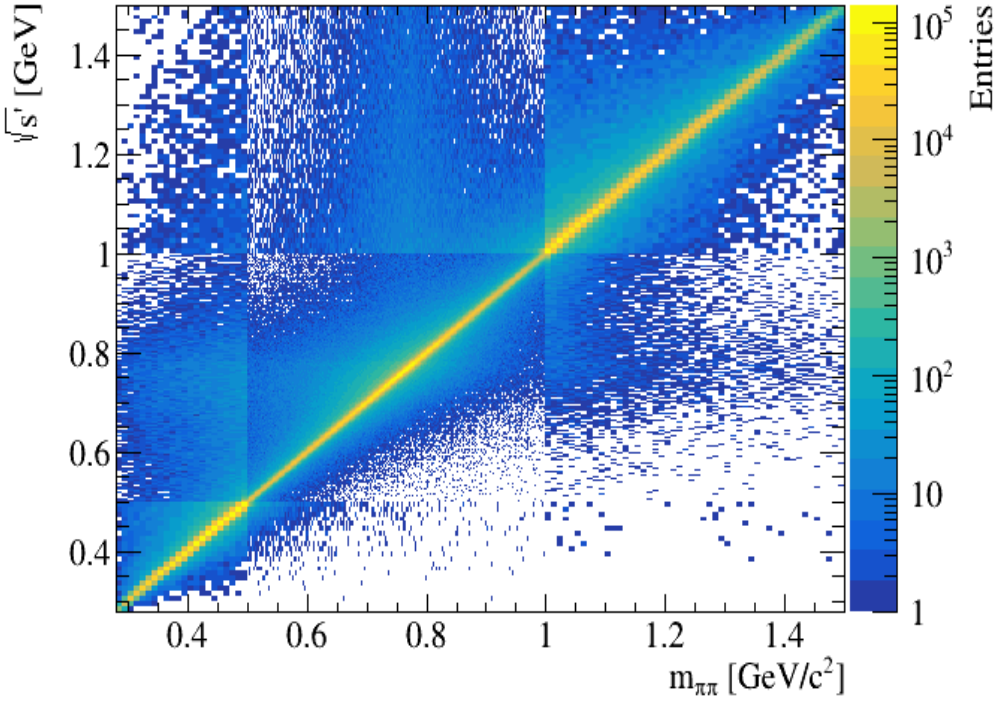

Muon unfolding

- Unfolding results with original MC (UR1) and with one iteration of truth−MC reweighting (UR2) show to be close to the initial data.
- Further iterations have negligible effect, and the unfolded spectrum remains stable, indicating a minimal systematic impact from mismodeling the generated mass distribution.
- MC reweighted (UR2) is used as the nominal unfolding result.

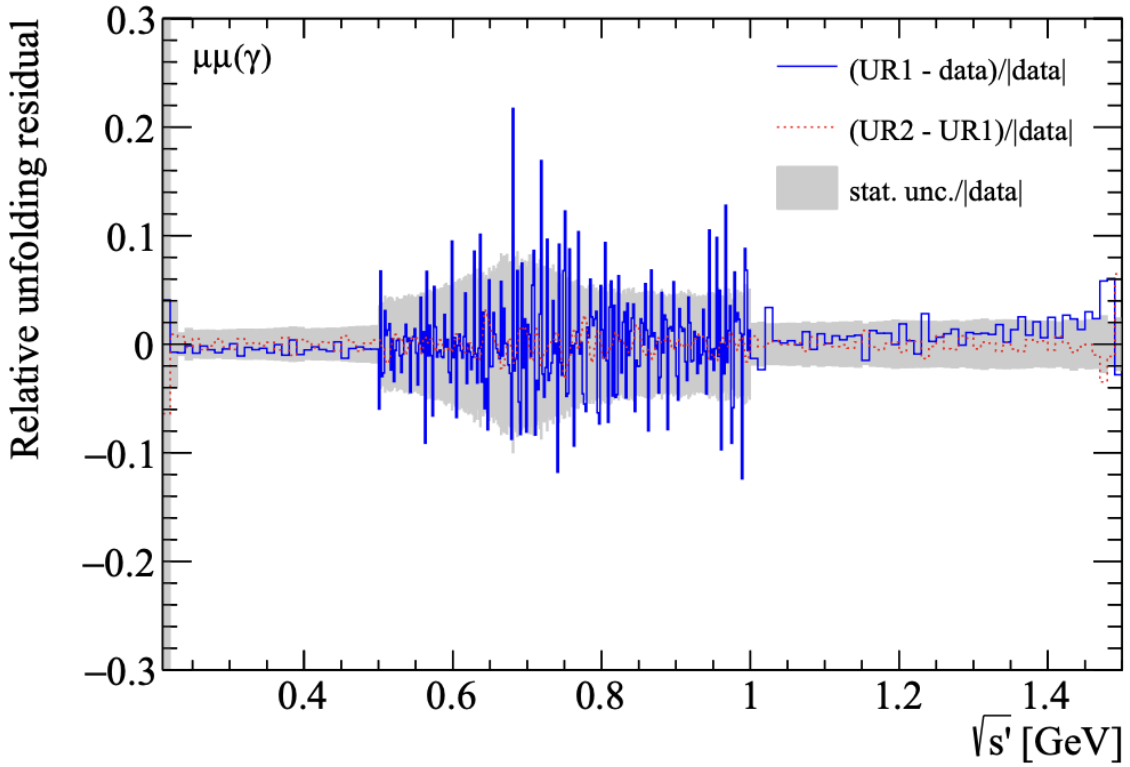

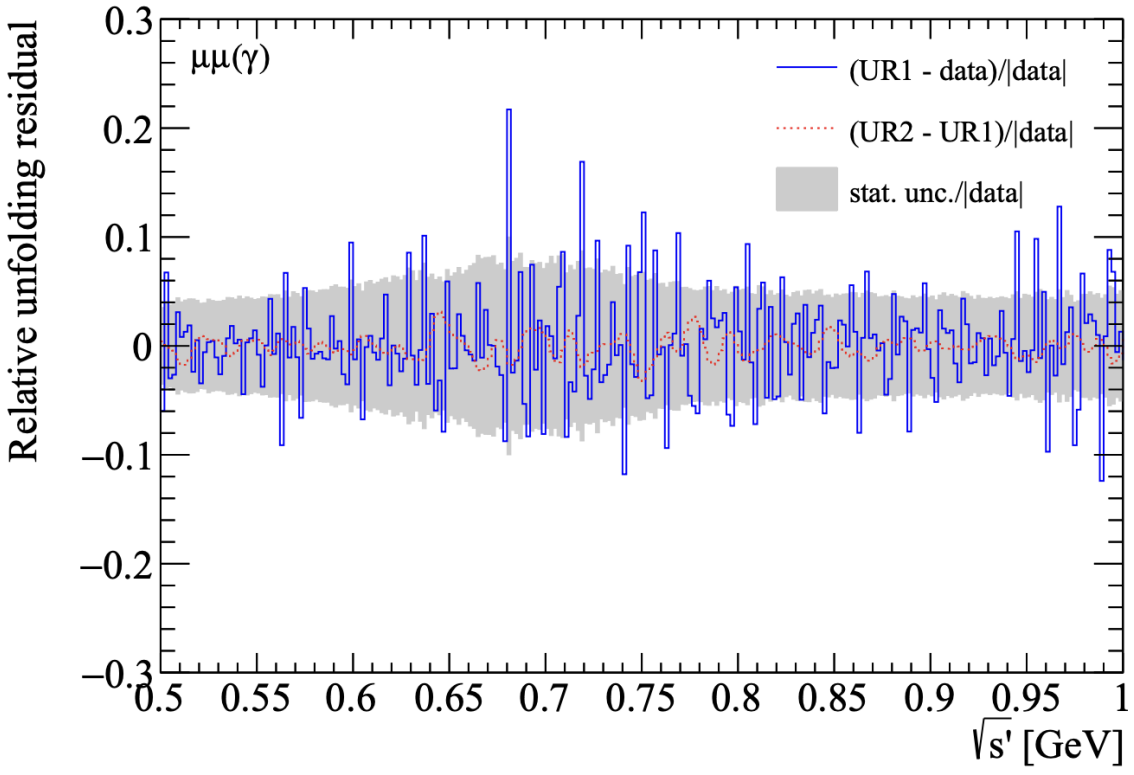

Muon uncertainties after unfolding

- Statistical uncertainties are estimated by **coherent** *Poisson* pseudo experiments of the data spectrum and the migration matrix.
- Systematic uncertainties propagated through coherent shifts of all bins for a given systematic source + unfolding + comparison with nominal spectrum ($\pm 1\sigma$ variations).
- Systematics are smoothed using a Gaussian kernel.
- Dominated by Trigger L3, tracking, vertex, 2D $-\ \chi^2$selection, etc.
- Statistical uncertainty below 5% under the ρ peak.

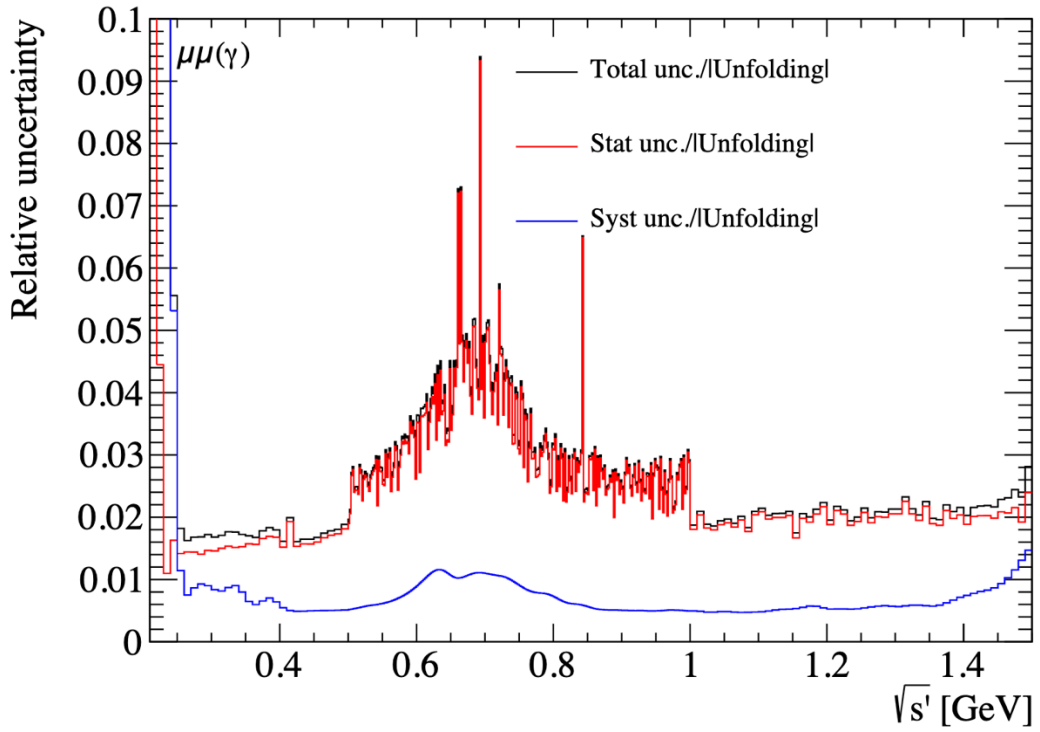

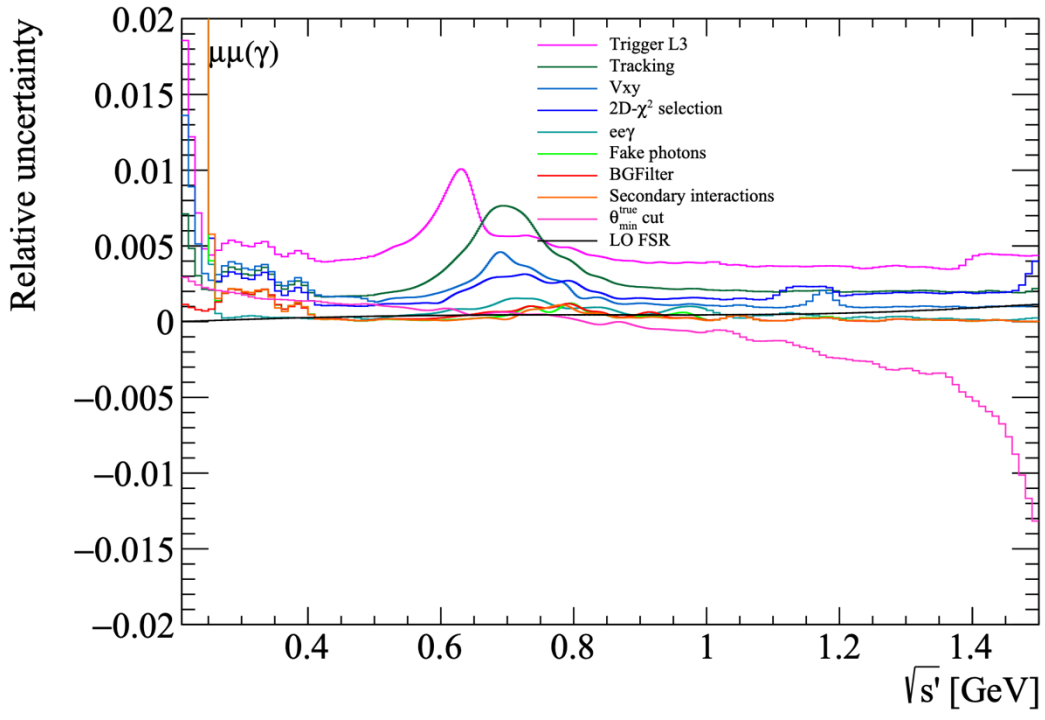

Pion unfolding

- Unfolding results (UR1 and UR2) show to be close to the initial data with more significant corrections in the $\rho - \omega$ interference region.
- Further iterations have negligible effect, and the unfolded spectrum remains stable, indicating a minimal systematic impact from mismodeling the generated mass distribution.
- MC reweighted (UR2) is used as the nominal unfolding result.

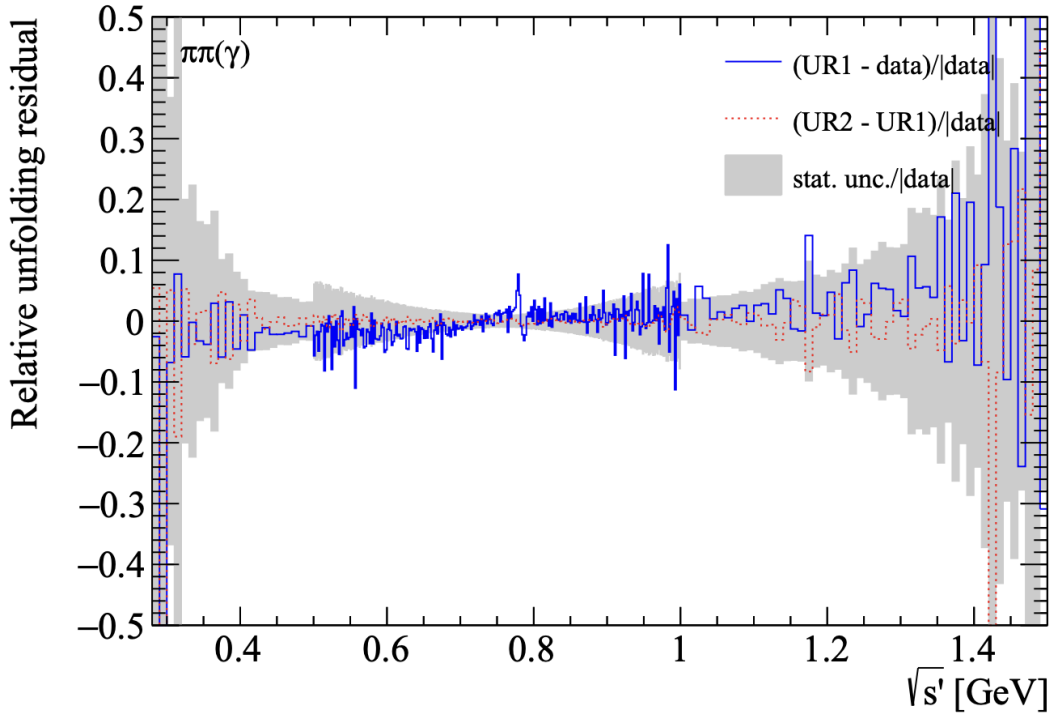

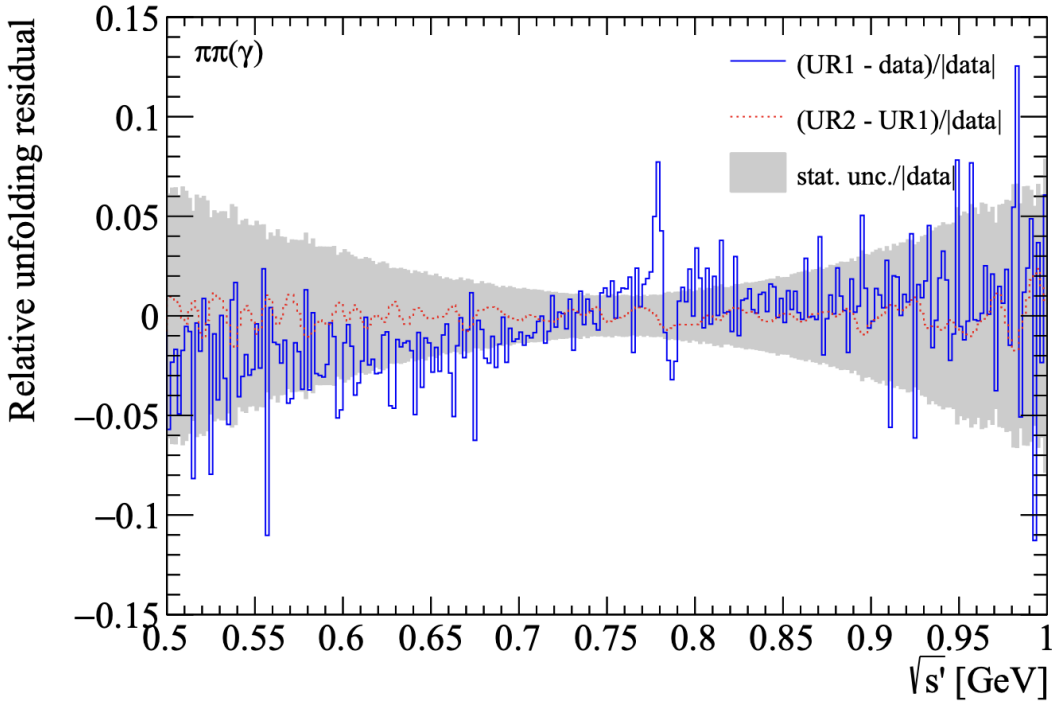

Pion uncertainties after unfolding

- Systematic uncertainties dominate at low and high mass while in the central region the statistical uncertainty dominates
- Systematic uncertainty is mainly dominated by Trigger L3, $\theta_{\mathrm{min}}^{\mathrm{true}}$ cut, tracking, etc.
- Statistical uncertainty below 1% around the $\rho - \omega$ interference.

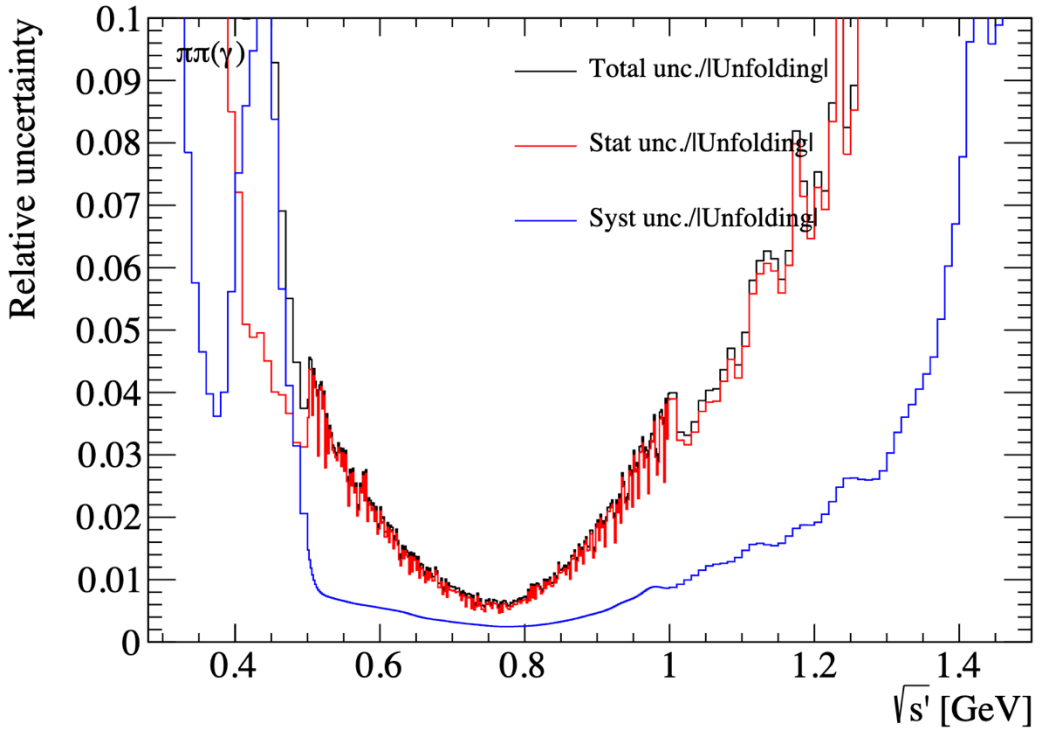

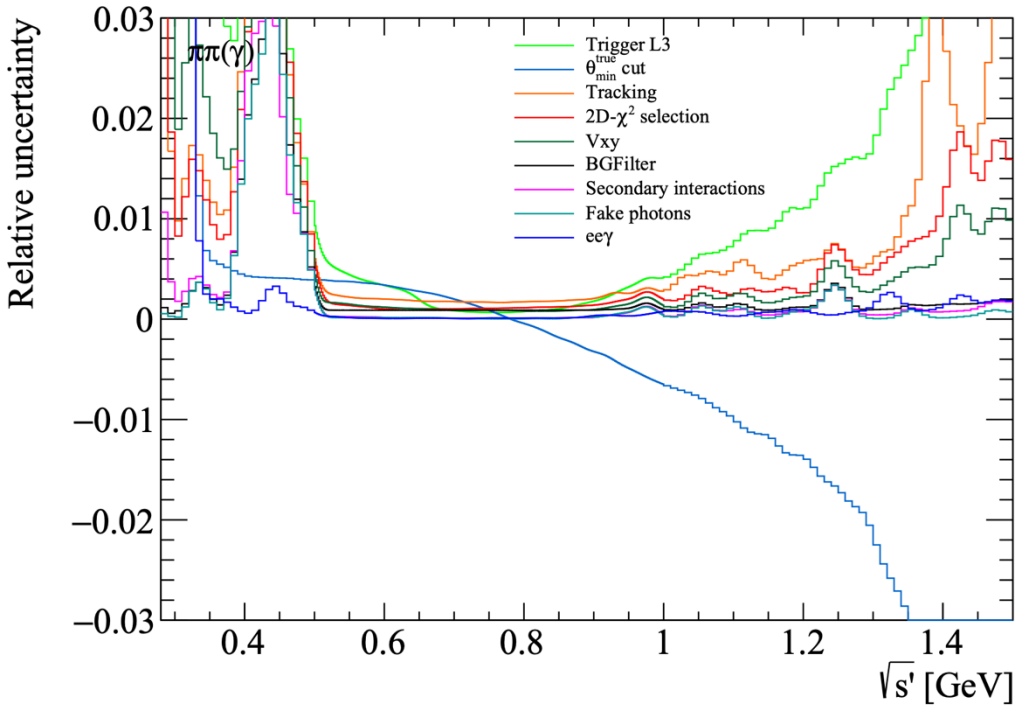

Effective ISR luminosity determination

- Effective ISR luminosity needed to extract ππ cross sections. Derived from the **muon channel.**

$$\frac{dL^{\text{eff}}_{\text{ISR}}}{d\sqrt{s'}} = \frac{dN^{\text{ISR}}_{\mu\mu}/d\sqrt{s'}}{\epsilon_{\mu\mu}(\sqrt{s'})\ \sigma^{0}_{\mu\mu}(\sqrt{s'})}$$

- where:
  - $\epsilon_{\mu\mu}$: acceptance of the selection for muons
  - $\sigma^{0}_{\mu\mu}$: Bare cross section $e^+e^- \to \mu^+\mu^-$
  - $dN^{ISR}_{\mu\mu}/d\sqrt{s'}$: Unfolded muon spectrum

- Ratio $(dN^{ISR}_{\mu\mu}/d\sqrt{s'})/\epsilon_{\mu\mu}$ is replaced by

$$\frac{dN^{\text{ISR}}_{\mu\mu}/d\sqrt{s'}}{\epsilon_{\mu\mu}(\sqrt{s'})} = \underbrace{\frac{dN^{\text{MC gen}}_{\mu\mu}}{d\sqrt{s'}}}_{\text{Phokhara spectrum at generation level}} \times \underbrace{(1 - f_{\text{LO FSR}})}_{\text{removes the LO FSR contribution}} \times \underbrace{f_{\mu\mu}(\sqrt{s'})}_{\text{2nd order polynomial fit to data/MC}}$$

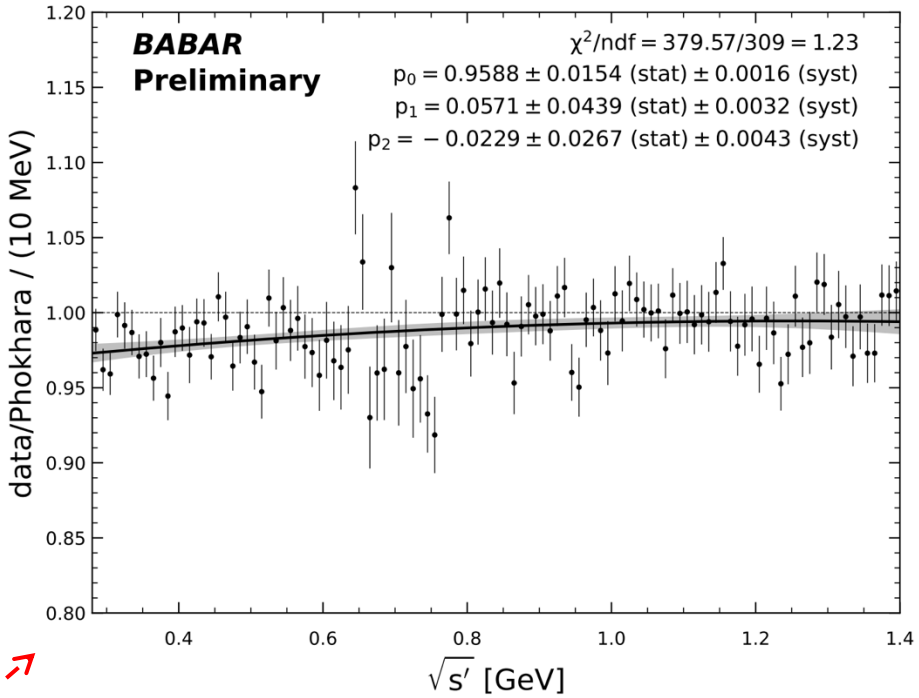

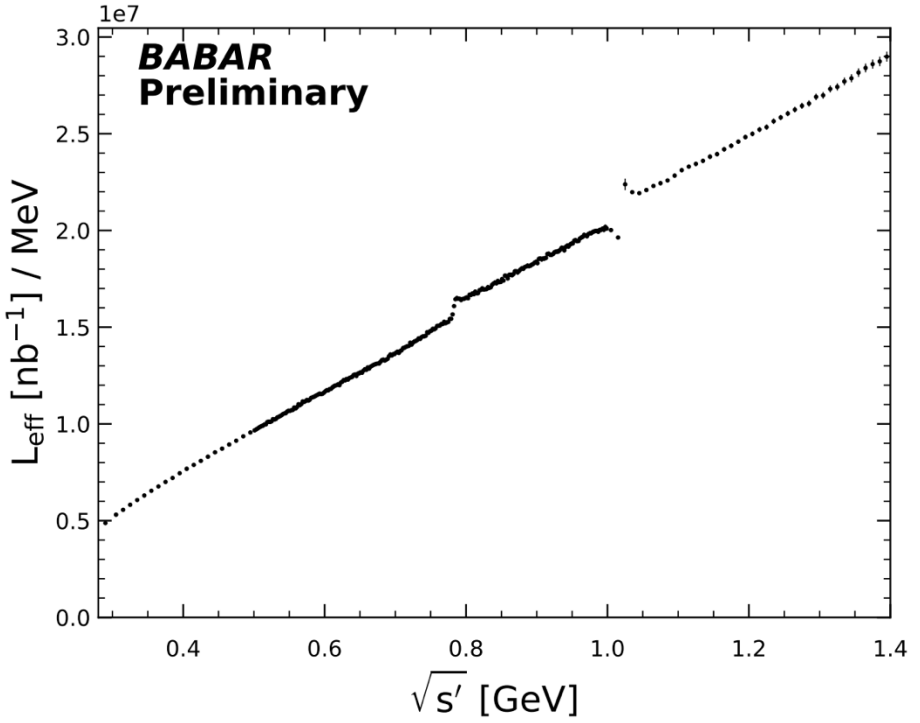

$\pi\pi$ cross section

$$\sigma^0_{\pi\pi}(\sqrt{s'}) = \frac{\frac{dN_{\pi\pi}}{d\sqrt{s'}}}{\epsilon_{\pi\pi}(\sqrt{s'})\frac{dL^{\text{eff}}_{\text{ISR}}}{d\sqrt{s'}}}$$

- Using the unfolding pion spectrum, detector acceptance vs $\sqrt{s'}$ and the effective ISR luminosity (from $\mu\mu$ channel) we obtain the cross section $\sigma^0_{\pi\pi}(\sqrt{s'})$.
- Reduced systematic uncertainties due to cancelling error sources or corrections common to $\mu\mu\gamma$ and $\pi\pi\gamma$.
- Clear $\rho - \omega$ interference structure

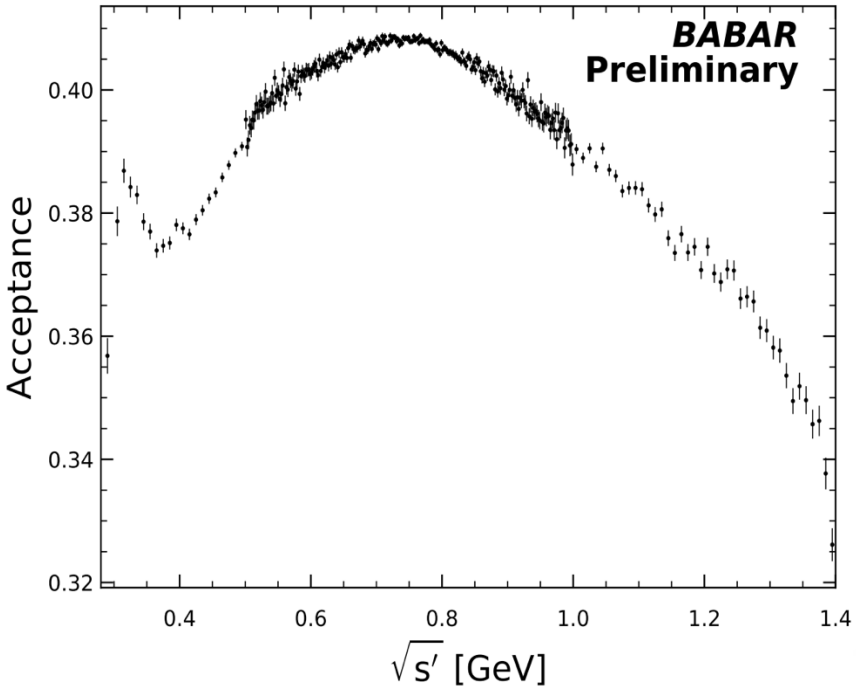

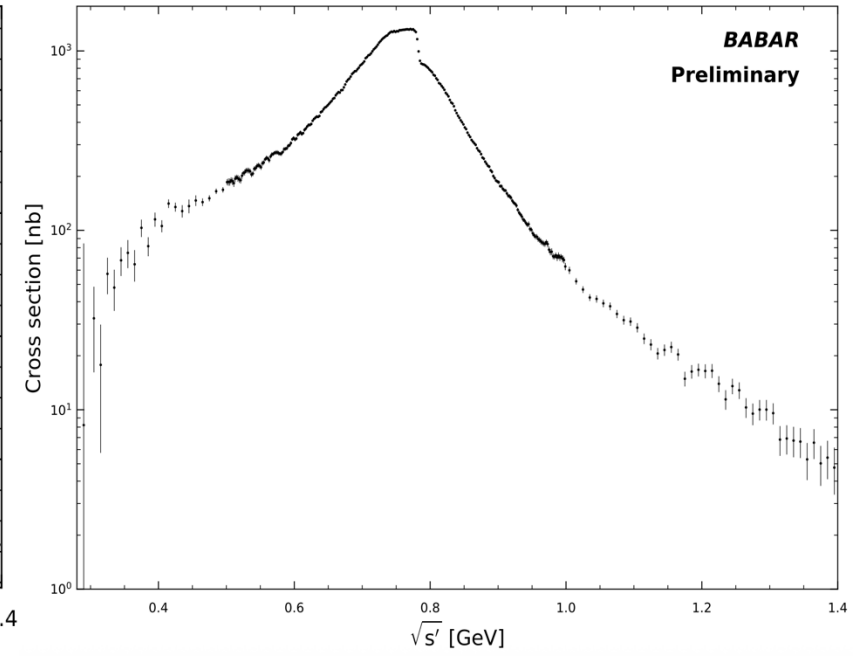

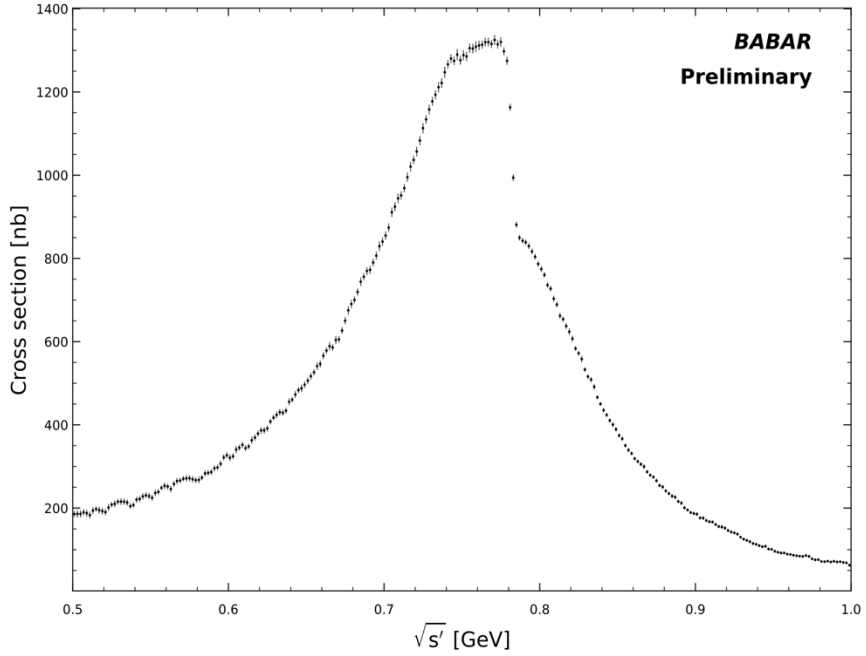

$\pi\pi$ contribution to a_μ

- 2025 results are in **excellent agreement** with 2009
- Best precision achieved in the $\rho - \omega$ interference region.
- Larger uncertainties at low/high masses due to muon background

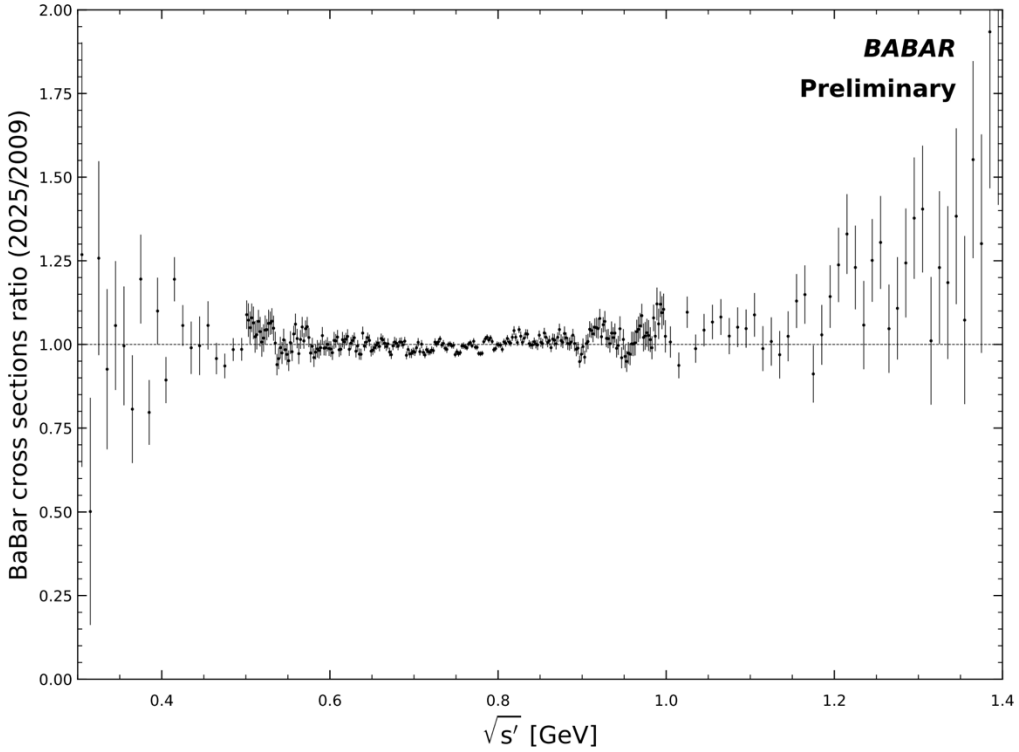

Energy range [GeV]	**2025** ($a_\mu^{\pi\pi} \pm$ **stat** $\pm$ **syst** $[10^{-10}]$)	**2009** ($a_\mu^{\pi\pi} \pm$ **stat** $\pm$ **syst** $[10^{-10}]$)
Below 0.5	$58.0 \pm 5.5 \pm 1.7$	$57.6 \pm 0.6 \pm 0.6$
0.5 – 1.4	$456.2 \pm 2.2 \pm 1.7$	$455.6 \pm 2.1 \pm 2.6$

Energy range [GeV]	**2025–2009 average (preliminary)** $a_\mu^{\pi\pi}$ $[10^{-10}]$
Below 0.5	58.2 ± 0.8
0.5 – 1.4	455.9 ± 2.1
Below 1.4	514.1 ± 2.5
Below 1.8 (1.4 – 1.8 from 2009)	514.4 ± 2.5

Summary and outlook

- New **blind BaBar analysis** (460 fb^{-1}) confirms the $\pi^+\pi^-$ contribution to a_μ.
- Independent method (angular fits, no PID) removes dominant 2009 systematic.
- Unblinded $\mu\mu\gamma$ spectrum agrees with QED, validating the approach.
- $\pi\pi$ cross section consistent with 2009, with **reduced systematics** in 0.5–1.4 GeV.

- Results:
  - Below 0.5 GeV: $a_\mu^{\pi\pi} = \left(58.0 \pm 5.5\,(\text{stat.}) \pm 1.7\,(\text{syst.})\right) \times 10^{-10}$
  - 0.5–1.4 GeV: $a_\mu^{\pi\pi} = \left(456.2 \pm 2.2\,(\text{stat.}) \pm 1.7\,(\text{syst.})\right) \times 10^{-10}$
- Robustness shown by excellent agreement with 2009.

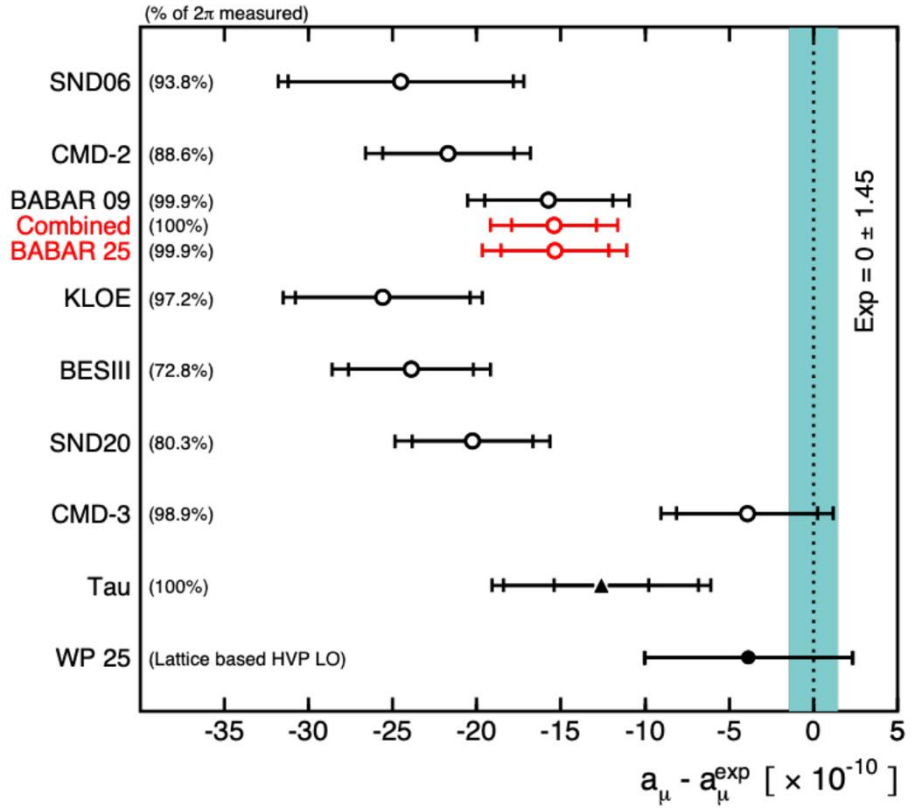

More information in Lepton Photon 2025 talks:
Léonard's talk : New precise measurement of the $e^+e^- \to \pi^+\pi^-(\gamma)$ cross section with BaBar
Zhiqing's talk : Review of HVP calculations via e^+e^- measurements

BACKUP

Getting a_μ from $e^+e^- \to \pi^+\pi^-(\gamma)$ cross section

- Cross section of $e^+e^- \to \pi^+\pi^-(\gamma)$ at reduced energy $\sqrt{s'} = m_{XX}$ (X = any final state) from measurement of $e^+e^- \to X\gamma_{ISR}$ with $E_{\gamma_{ISR}}$ energy in center of mass (CM) frame.
- Measuring the yield $N_{X\gamma_{ISR}}$ gives the bare cross section $\sigma_X^0(\sqrt{s'})$ (excluding vacuum polarization)

$$\frac{dN_{X\gamma}}{d\sqrt{s'}} = \frac{dL_{\text{ISR}}^{\text{eff}}}{d\sqrt{s'}}\ \varepsilon_{X\gamma}(\sqrt{s'})\ \sigma_X^0(\sqrt{s'}) \tag{1}$$

- $\varepsilon_{X\gamma}$= detection efficiency in acceptance → from simulation with data corrections.
- L_{ISR}^{eff} = effective ISR luminosity → from $X = \mu\mu(\gamma_{FSR})$ in (1) and $\sigma_X^0(\sqrt{s'})$ taken from QED computation
- Ratio of $\pi\pi$ and $\mu\mu$ mass spectra ⇒ cancellation of VP⇒ ratio of (1)

$$\frac{\sigma^0_{\pi\pi(\gamma_{\text{FSR}})}(\sqrt{s'})}{\sigma_{\text{pt}}(\sqrt{s'})(1+\delta^{\mu\mu}_{\text{FSR}})(1+\delta^{\mu\mu}_{\text{add. FSR}})} \tag{2}$$

- $\sigma_{pt}(\sqrt{s'}) = 4\pi\alpha^2/3s'$: cross section for point-like charged fermions
- $\left(1+\delta^{\mu\mu}_{(add.)\,FSR}\right)$: corrections for lowest-order(additional) FSR contributions.
- Dispersion relation with QED kernel $K(s')$:

$$a_\mu^{\pi\pi(\gamma_{\text{FSR}}),\,\text{LO}} = \frac{1}{4\pi^3}\int_{4m_\pi^2}^{\infty} ds'\ K(s')\ \sigma^0_{\pi\pi(\gamma_{\text{FSR}})}(s') \tag{3}$$

NLO fits description

- Use measured ISR energy/direction + momenta/angles of both tracks.

- $\boldsymbol{\gamma_{ISR}\gamma_{LA}}$ **fit:** additional large angle (LA) γ with respect to the beams (0.35 − 2.45 rad).
- $\boldsymbol{\gamma_{ISR}\gamma_{SA}}$ **fit:** additional small angle (SA) γ fitted assuming collinearity with one of the beams.
- **NLO LA sample:** $\chi^2_{\mathrm{LA}} < \chi^2_{\mathrm{SA}}$, $\mathrm{E}_{\gamma,\mathrm{LA}} > 200$ MeV.
- **NLO SA sample:** $\chi^2_{\mathrm{LA}} > \chi^2_{\mathrm{SA}}$, $\mathrm{E}^*_{\gamma,\mathrm{SA}} > 200$ MeV.
- **LO sample:** events below the thresholds.
- Larger background in $\pi\pi\gamma$ process, suppressed with
- optimized BDT-based 2D $-\ \chi^2$ selection (98-99% efficiency).

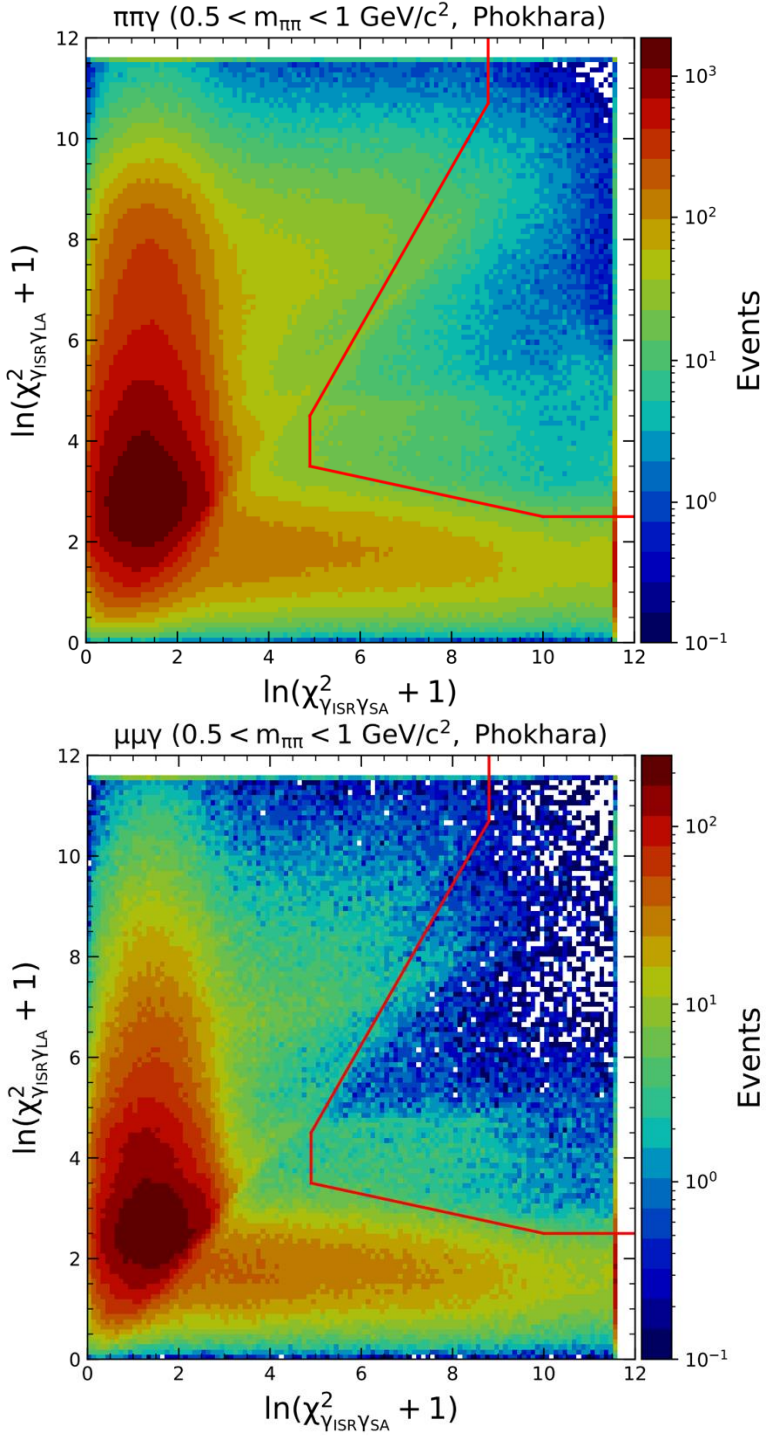

Cut-based selection of $ee\gamma$ events

- Cut-based selection studied in a previous analysis (2015):

$$\left(\frac{E_{\text{cal}}}{p}\right)_1 > 0.5, \quad \left(\frac{dE}{dx}\right)_1 > 600,$$
$$\left(\frac{dE}{dx}\right)_2 > 550 + 60 \times p_2 + 8.9 \times p_2^2 ,$$
$$\text{isElectron}_{1/2} = \left(\frac{E_{\text{cal}}/p - 1}{0.15}\right)^2 + \left(\frac{dE/dx - 690}{150}\right)^2 < 10$$

- For 1 (2) the track with the highest (lowest) momentum.

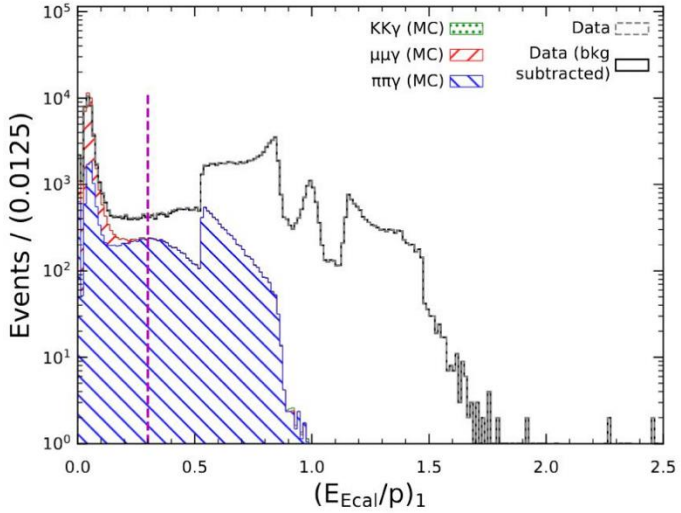

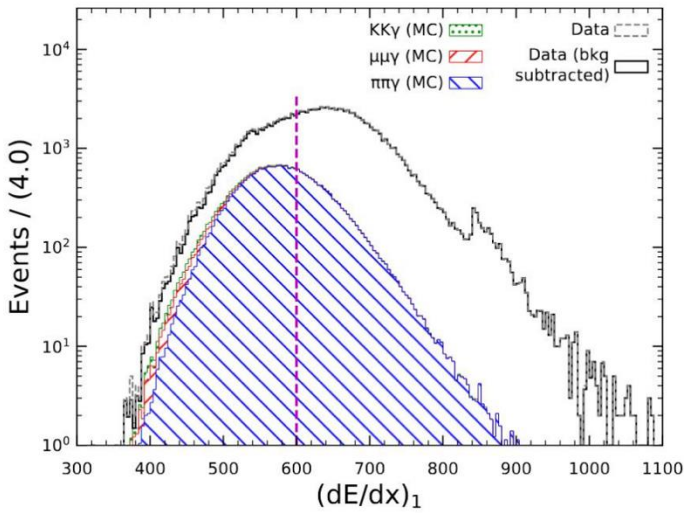

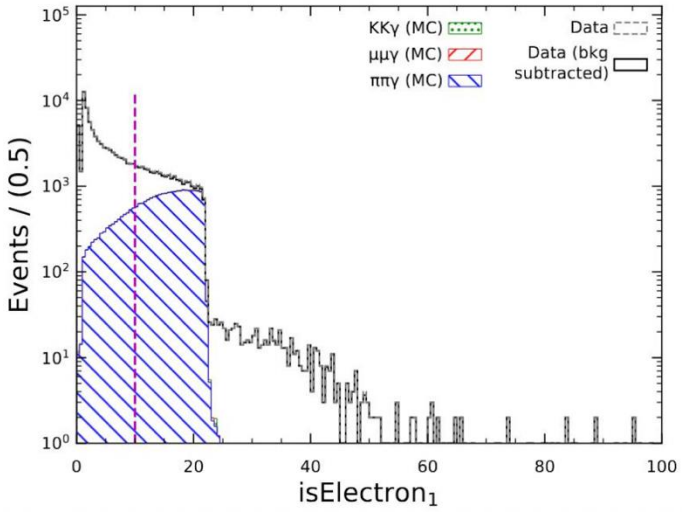

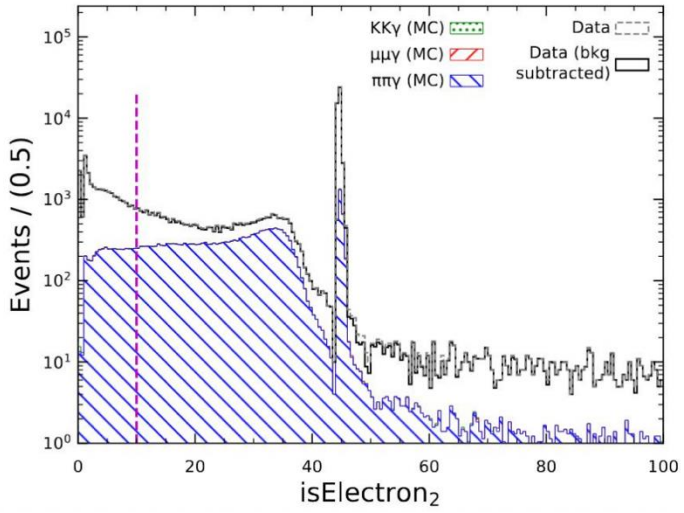

BDT-based selection of $ee\gamma$ events

- Additional selection performed using a BDT implemented with the XGBoost library, trained on the following variables:

$$(E_{\mathrm{Ecal}}/p)_1,\ (dE/dx)_{1/2},\ p_{1/2},\ \mathrm{isElectron}_{1/2},\ V_{xy},\ m_{\pi\pi},\ m_{\mu\mu}$$

- Training is carried out on events that pass the cut-based selection, with real data used as signal and Monte Carlo as background.
- BDT hyperparameters (tree depth and learning rate) are optimized to maximize classification accuracy.
- To avoid bias, two independent BDTs are trained on separate halves of the dataset, with each applied to the opposite half.
- The training uses the logarithmic loss function as the evaluation metric, and early stopping is applied to prevent overfitting.
- The output of the classifier is the probability that an event corresponds to signal (i.e., $ee\gamma$-like).

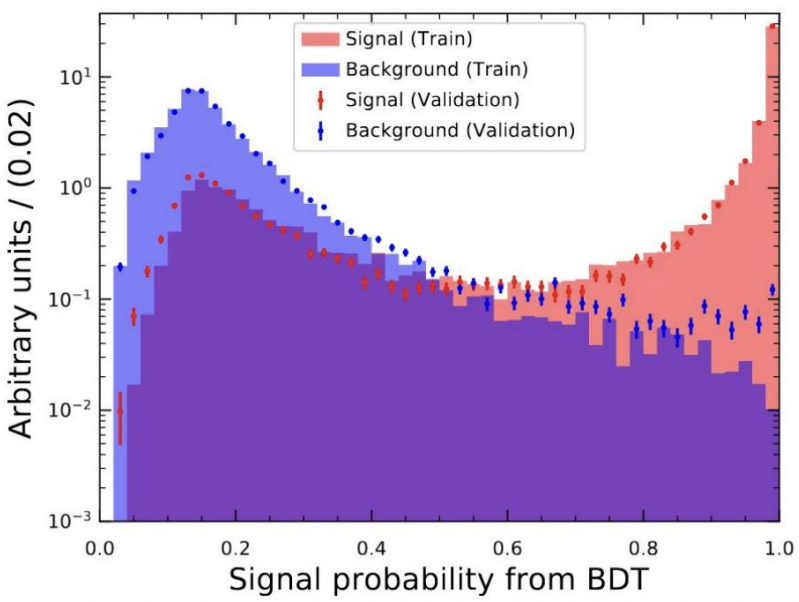

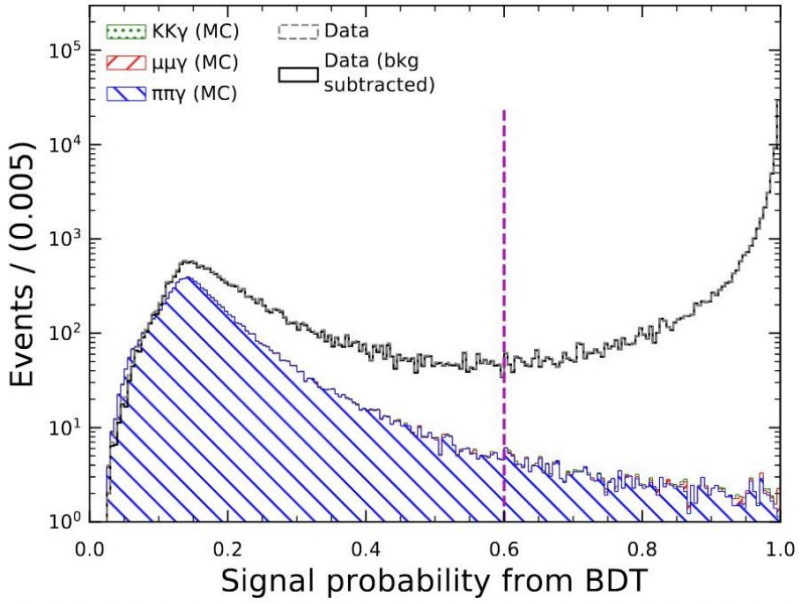

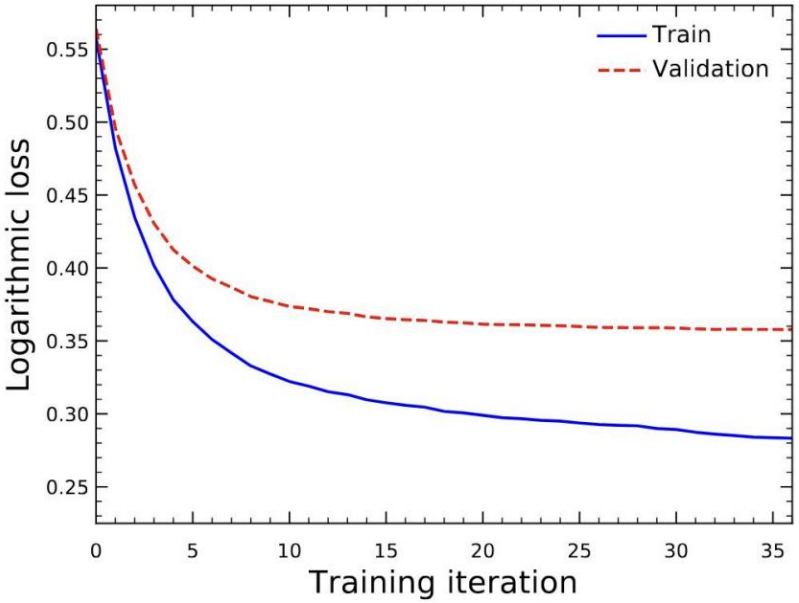

Tracking efficiency corrections on muons

- **2009 formalism:** tag-and-probe method with single track reconstructed + second track predicted from 1-constraint kinematic fit (method 1).
- Poor resolution on predicted parameters of low-momentum tracks and/or at edge of acceptance: alternative, 4-constraint fit (method 2), ignoring predicted probe track parameters.
- <u>Tracking correction:</u>

$$C_{\text{tracking}} = \frac{[(1 - f_0 - f_3)\epsilon^2]_{\text{data}}}{[(1 - f_0 - f_3)\epsilon^2]_{\text{MC}}}$$

- ϵ: average track efficiency
- f_0: 2-track correlated loss probability
- f_3 : extra reco track loss probability

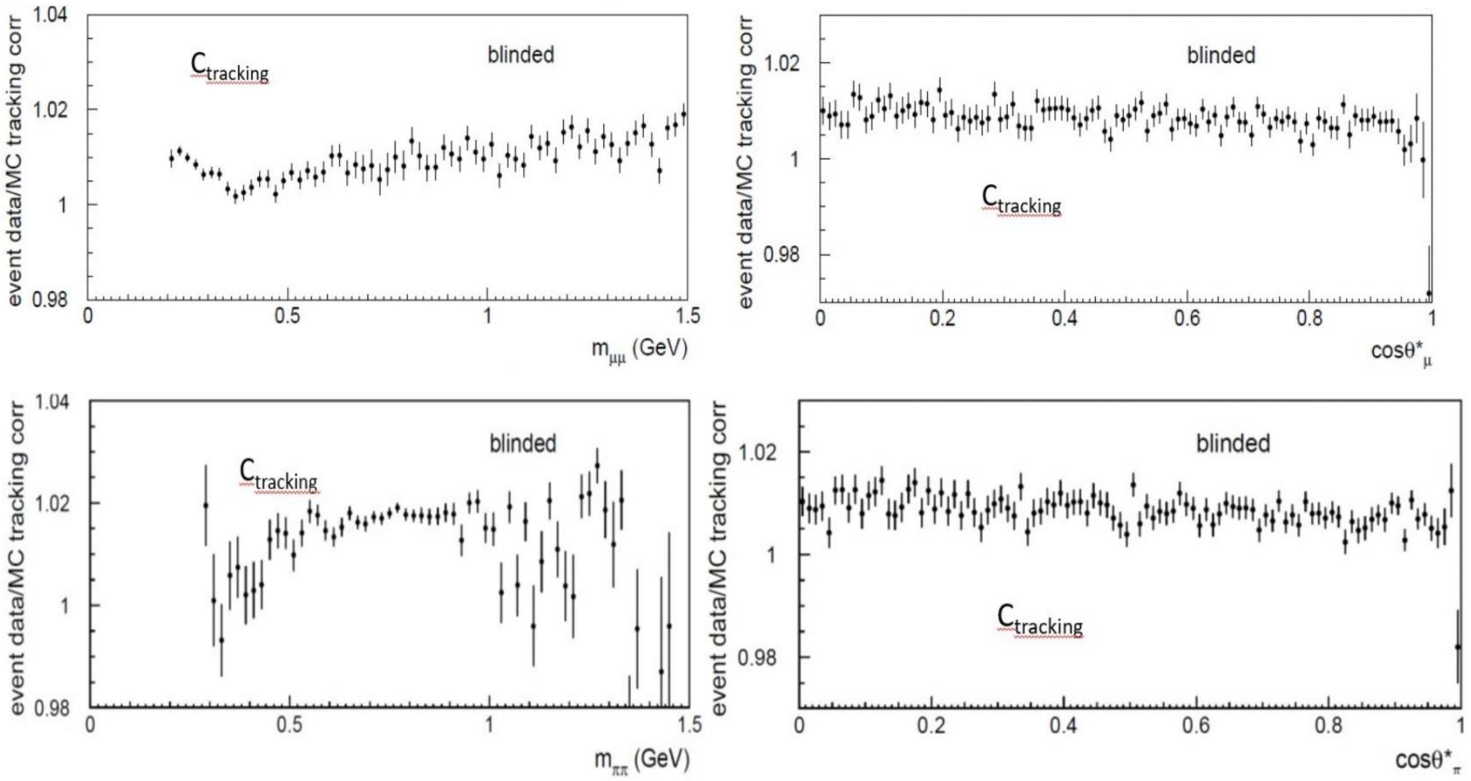

Angular fit

- Neymann and Pearson χ^2 were also considered, CNP was retained.
- Carried out by a Combined Neymann-Pearson χ^2
  - j: $|\cos\theta^*|$ bin.
  - M_j: observed events in a given bin (data).
  - N_j: probability model (predicted events).
  - ΔN_j: Statistical error in N_j.

$$\chi^2_{\mathrm{CNP}} = \sum_j \frac{(M_j - N_j)^2}{3/\left(\frac{1}{M_j+(\Delta N_j)^2} + \frac{2}{N_j+(\Delta N_j)^2}\right)}$$

- Where the probability model is a linear combination of templates

$$N = M\left[\sum_{i=1}^{k-1} f_i x_i + \left(1 - \sum_{i=1}^{k-1} f_i\right) x_k\right] \pm M\sqrt{\sum_{i=1}^{k-1} (f_i \Delta x_i)^2 + \left[\left(1 - \sum_{i=1}^{k-1} f_i\right) \Delta x_k\right]^2}$$

- M : integral over $|\cos\theta^*|$ of the fitted data distribution in a mass bin,
- $f_i \in [0,1]$: parameters of fit, scale factors of templates with $\sum_i f_i = 1$

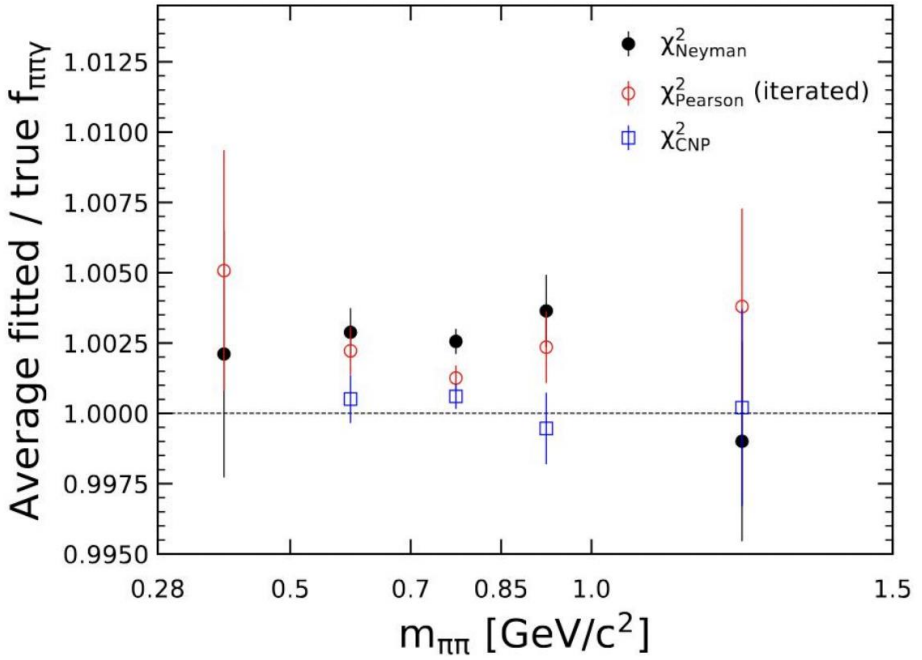

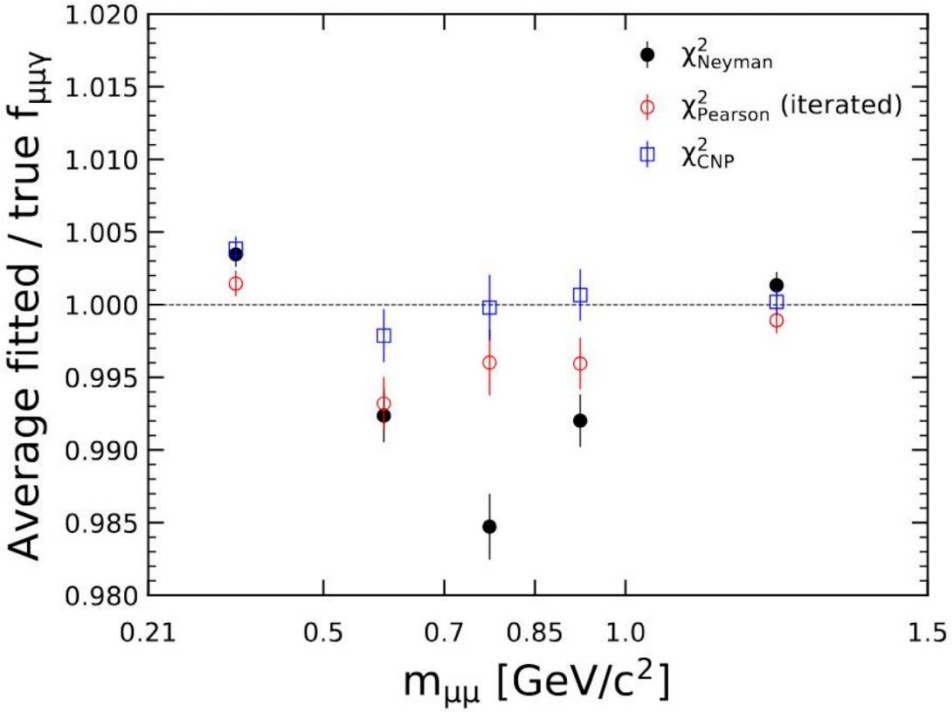

FSR region

- BaBar has a large acceptance to measure ISR Large Angle (LA) photons.
- We define the "nominal" using $\theta_{\min}^{\text{true}} < 20°$.
- Different angle cuts were considered: $\theta_{\min}^{\text{true}} = [10,15,20,25]$

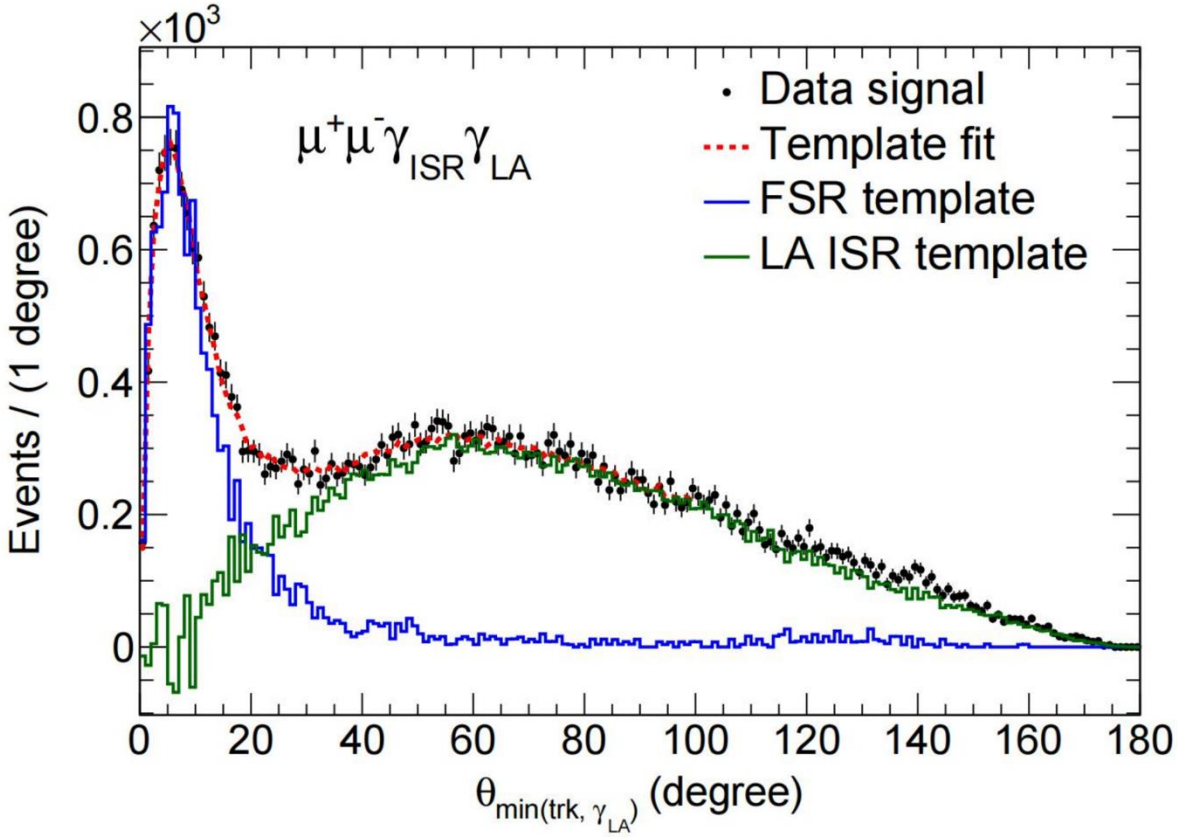

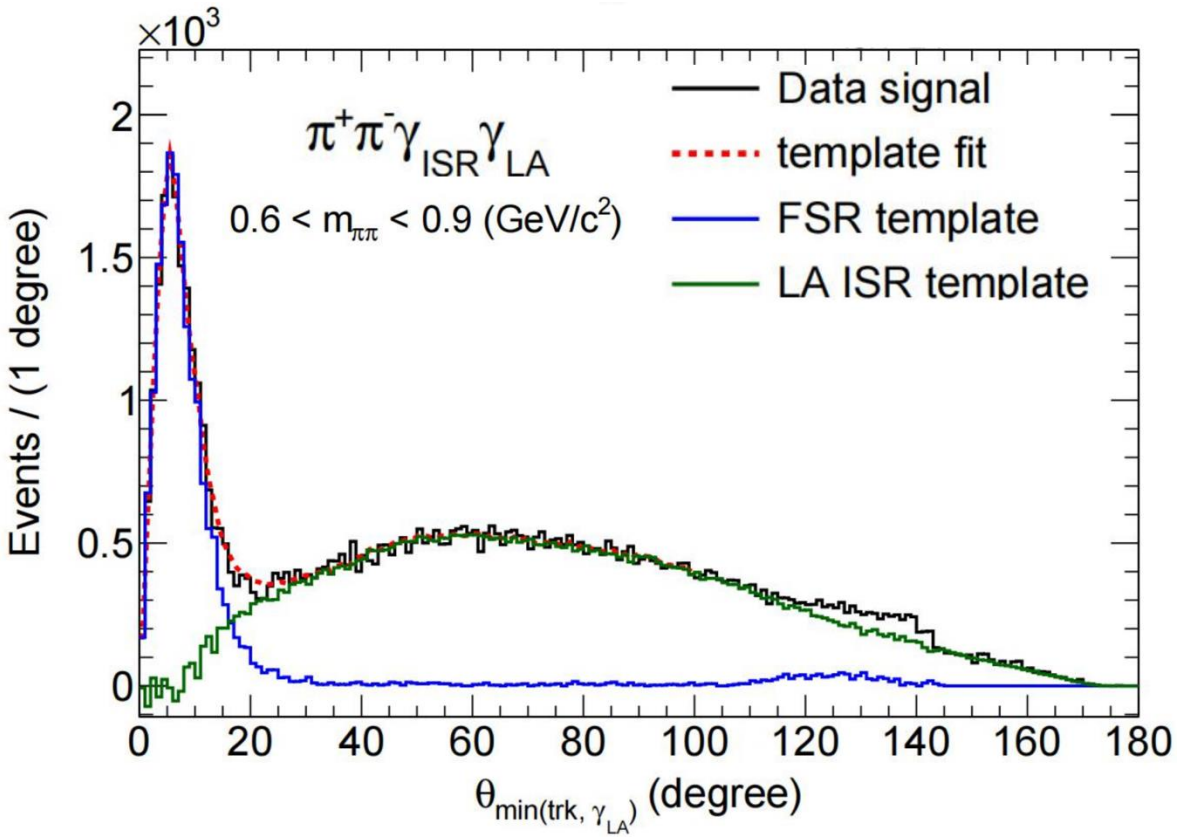

$m_{\pi\pi}$ vs Unfolding spectrum